Ann. Inst. H. Poincaré D
Comb. Phys. Interact. (Online first)
DOI 10.4171/AIHPD/169

Dyson–Schwinger equations in minimal subtraction

Paul-Hermann Balduf

Abstract. We compare the solutions of one-scale Dyson–Schwinger equations (DSEs) in the minimal subtraction (MS) scheme to the solutions in kinematic momentum subtraction (MOM) renormalization schemes. We establish that the MS-solution can be interpreted as a MOM-solution, but with a shifted renormalization point, where the shift itself is a function of the coupling. We derive relations between this shift and various renormalization group functions and counterterms in perturbation theory. As concrete examples, we examine three different one-scale Dyson–Schwinger equations: one based on the 1-loop multiedge graph in $D = 4$ dimensions, one for $D = 6$ dimensions, and one for mathematical toy model. For each of the integral kernels, we examine both the linear and nine different non-linear Dyson–Schwinger equations. For the linear cases, we empirically find exact functional forms of the shift between MOM and MS renormalization points. For the non-linear DSEs, the results for the shift suggest a factorially divergent power series. We determine the leading asymptotic growth parameters and find them in agreement with the ones of the anomalous dimension. Finally, we present a tentative exact solution to one of the non-linear DSEs of the toy model.

1. Introduction

1.1. Motivation

So far, the systematic Hopf-algebraic treatment [3–5, 27, 29, 31, 44, 45] of Dyson–Schwinger equations (DSEs) [24,40] has relied on kinematic (MOM) renormalization schemes. The solution of a DSE is the renormalized Green function $G(p^2)$. MOM schemes assign a value to the renormalized Green function $G(p^2)$ at one particular momentum $p^2 = \mu^2$, and thereby have a transparent interpretation as boundary condition for the DSE. For a single (non-coupled) DSE, the only remaining unknown object is the anomalous dimension $\gamma(\alpha)$ as a function of the renormalized coupling α. If MOM-conditions are used systematically, explicit regularization of divergent integrals is not necessary [29, 31] and one only deals with finite quantities at all stages.

2020 Mathematics Subject Classification. Primary 81T15; Secondary 81T17, 16T30, 40G10.
Keywords. Dyson–Schwinger equation, renormalization scheme, minimal subtraction, non-perturbative correction, anomalous dimension.

In fact, $\gamma(\alpha)$ can be computed from a differential equation without any divergent integral. The earlier works [22, 23] do regulate the integrals explicitly using dimensional regularization [6, 43], but they use MOM renormalization conditions nonetheless.

On the other hand, many perturbative computations in quantum field theory use the combination of dimensional regularization and minimal subtraction (MS) renormalization conditions. In this scheme, all singular terms in the regulator ε are subtracted, but the resulting amplitude does not respect any particular kinematic boundary condition. The MS-solution of a DSE can only be found by explicitly regulating and renormalizing the divergent integrals at each loop order.

At the same time, different renormalization schemes should not lead to different physical outcomes, therefore, there ought to be *some* particular momentum $\widehat{\mu}$ such that minimal subtraction agrees with kinematic renormalization using that very reference momentum $\widehat{\mu}$. Indeed, the existence of this correspondence is proven on an abstract algebraic level [30, 38]. Finding the explicit relationship is of practical relevance since the perturbative solution is typically only known to a few orders. In that case, the truncated MS-renormalized results are truly different from the MOM ones and a priori only valid around their respective renormalization points [15]. Knowing the physical value of the MS-renormalization point $\widehat{\mu}$ is then crucial for the validity range of the truncated Green function. Furthermore, renormalization group functions differ between both schemes. In MS, but presumably not in MOM, the beta function is expected to be dominated by subdivergence-free diagrams [35]. A more concrete understanding of the relation between MOM and MS can help to translate such conjectures to the other scheme and subsequently attack them with a different set of tools.

1.2. Content

The present paper begins in Section 2 with a pedagogical discussion of Z-factors and renormalization group equations in both MOM and MS and their various relations and identities. In Section 3, we establish that, in the physical limit $\varepsilon \to 0$, the Green function in MS can be interpreted as a MOM Green function with shifted renormalization point. We derive several ways to compute this shift.

In the remainder, we analyse propagator-type Dyson–Schwinger equations based on three different primitive integral kernels. The first one is the 4-dimensional bubble (= 1-loop-multiedge) graph appearing, e.g., in the fermion propagator in Yukawa theory. The second one is the same graph in 6 dimensions, contributing to the ϕ^3-propagator, and the third is a mathematical toy model which has occasionally been used to study renormalization. In all three cases, we consider the recursive insertion of the Green function into only one place in the kernel graph.

First, we insert the Green function itself, which amounts to a linear DSE known as the rainbow approximation. In Section 4, the algorithm for linear DSEs is developed

for the case of the 4-dimensional bubble integral. Subsequently, this is applied to the $D = 6$ case in Section 5 and to the toy model in Section 6. As a counterexample, we demonstrate in Section 7 that the chain-approximation, not arising from a DSE, does not allow for a shift between MS and MOM.

Secondly, we insert the Green function raised to a power $\in \{-4, \ldots, +6\}$, producing non-linear DSEs. In Section 8, the algorithm for non-linear DSEs is explained and used for the 4-dimensional model. The last Sections 9 and 10 contain the results for the non-linear DSEs for the two remaining models, $D = 6$ and the toy model. Section 11 is a summary of the results.

2. Theoretical background

2.1. Unrenormalized Dyson–Schwinger equation

We consider DSEs of the form

$$G_0(\alpha_0, x) = 1 + \alpha_0 \int \mathrm{d}y \; K(x, y) Q(G_0(\alpha_0, y)) G_0(\alpha_0, y), \tag{2.1}$$

where $G_0(\alpha_0, x)$ is the unrenormalized Green function and $K(x, y)$ is an integral kernel, determined by a single primitive Feynman diagram. Restricting the Green function to depend on only one single external scale x, means that $G_0(\alpha_0, x)$ represents a 1PI 2-point-function and $K(x, y)$ stems from a propagator-type diagram. For a more general Green function, one needs to include also scale-less "angle" variables [13]. The variable $x := p^2/\mu^2$ is the external momentum scaled to some fixed reference momentum μ. In the literature, propagator-type DSEs are often written with a minus sign, $G = 1 - \alpha \int \ldots$ We will use a plus for all DSEs considered in this work.

In the cases we consider, the invariant charge is a monomial of the Green function,

$$Q(G_0(\alpha_0, x)) = (G_0(\alpha_0, x))^s. \tag{2.2}$$

2.2. Renormalization

Carrying out renormalization on an integral- (rather than integrand-)level requires us to regulate the divergent integrals. In dimensional regularization [6, 43], the space-time dimension is changed by a non-integer shift ε, we choose $D = 4 - 2\varepsilon$ or $D = 6 - 2\varepsilon$. The unrenormalized amplitude of a finite graph is then a Laurent series in the regularization parameter ε.

We will only consider DSEs of multiplicatively renormalizable theories. This means that it is possible to eliminate all divergences at order m by two counterterms

$Z_G^{(m)}$ and $Z_\alpha^{(m)}$. They act as a rescaling of the Green function and the coupling constant according to

$$\begin{aligned} \alpha_0 &= Z_\alpha(\alpha,\varepsilon)\mu^{2\varepsilon}\cdot\alpha, \\ G(\alpha,\varepsilon,x) &= Z_G(\alpha,\varepsilon)\cdot G_0(Z_\alpha(\alpha,\varepsilon)\alpha,\varepsilon,x). \end{aligned} \tag{2.3}$$

These Z-factors are themselves functions of the renormalized coupling α and of the regularization parameter ε.

Renormalization of the coupling constant is only necessary if the theory has a non-vanishing beta function or, equivalently, a running coupling. See [32] for a recent account. Eventually, Z_α is given by the renormalization of the invariant charge Q. In the present case where there is only one Green function $G(\alpha,x)$ which needs renormalization, the invariant charge (2.2) leads to the identity

$$Z_\alpha(\alpha,\varepsilon) = (Z_G(\alpha,\varepsilon))^s. \tag{2.4}$$

The derivative of the renormalized coupling constant with respect to the renormalization point, at fixed unrenormalized coupling α_0, is the beta function of the theory,

$$\beta(\alpha,\varepsilon) := \mu^2\frac{\partial}{\partial\mu^2}\ln\alpha(\alpha_0,\mu) + \varepsilon = \frac{-\varepsilon}{\alpha\frac{\partial}{\partial\alpha}\ln(\alpha\cdot Z_\alpha(\alpha,\varepsilon))} + \varepsilon. \tag{2.5}$$

The anomalous dimension, on the other hand, is defined as the derivative of the renormalized Green function at fixed α_0, using equation (2.4) one finds

$$\gamma(\alpha,\varepsilon) := \mu^2\frac{\partial}{\partial\mu^2}\ln G(\alpha,\varepsilon) = (\beta(\alpha,\varepsilon)-\varepsilon)\alpha\frac{\partial}{\partial\alpha}\ln Z_G(\alpha,\varepsilon). \tag{2.6}$$

Note that sometimes, γ is defined as the derivative of the inverse (i.e., connected, not 1PI) 2-point Green function, or as the derivative with respect to μ. These definitions are equivalent up to overall signs and factors.

Conversely, the renormalization group functions $\beta(\alpha,\varepsilon)$ and $\gamma(\alpha,\varepsilon)$ uniquely determine the counterterms via

$$\begin{aligned} Z_\alpha(\alpha,\varepsilon) &= \exp\Big(-\int_0^\alpha \frac{\mathrm{d}u}{u}\frac{\beta(u,\varepsilon)}{\varepsilon-\beta(u,\varepsilon)}\Big), \\ Z_G(\alpha,\varepsilon) &= \exp\Big(-\int_0^\alpha \frac{\mathrm{d}u}{u}\frac{\gamma(u,\varepsilon)}{\varepsilon-\beta(u,\varepsilon)}\Big). \end{aligned} \tag{2.7}$$

Such relations have long been known in the traditional formulation ("Gross–'t Hooft relations") [16, 25, 42] as well as in the Hopf-algebraic formulation ("scattering type formula") of quantum field theory (see [18] and [19, Section 7]).

It follows from the above definitions that the renormalized Green function G fulfils—even for $\varepsilon \neq 0$ and not only in MOM renormalization—the Callan–Symanzik equation (CSE) [14,41]

$$(\gamma(\alpha,\varepsilon) + (\beta(\alpha,\varepsilon) - \varepsilon)\alpha\partial_\alpha)G(\alpha,\varepsilon,x) = x\partial_x G(\alpha,\varepsilon,x). \tag{2.8}$$

The renormalization group functions β, γ as well as the renormalized Green function are generally non-trivial functions of the regularisation parameter ε. Assuming that counterterms (2.3) are chosen properly, their limits at $\varepsilon \to 0$ exist:

$$\begin{aligned} \beta(\alpha) &:= \lim_{\varepsilon\to 0} \beta(\alpha,\varepsilon), \\ \gamma(\alpha) &:= \lim_{\varepsilon\to 0} \gamma(\alpha,\varepsilon), \\ G(\alpha,x) &:= \lim_{\varepsilon\to 0} G(\alpha,\varepsilon,x). \end{aligned} \tag{2.9}$$

These limits are usually implied when talking about the renormalized quantities. If the invariant charge has form (2.2) and consequently equation (2.4) holds, then by equation (2.7)

$$\beta(\alpha,\varepsilon) = s\cdot\gamma(\alpha,\varepsilon) \Rightarrow \beta(\alpha) = s\cdot\gamma(\alpha). \tag{2.10}$$

To directly compute the renormalization constants and renormalized solution from a DSE, one inserts equation (2.1) into equation (2.3) and uses equations (2.2) and (2.4) to obtain

$$\begin{aligned} G(\alpha,x) &= Z_G\Big(1 + Z_\alpha\alpha\int \mathrm{d}y\; K(x,y)(G_0(Z_\alpha\alpha,y))^{s+1}\Big) \\ &= Z_G + \alpha\int \mathrm{d}y\; K(x,y)Q(G(\alpha,y))G(\alpha,y). \end{aligned} \tag{2.11}$$

This equation can be solved iteratively by inserting the solution of order $(m-1)$, $G^{(m-1)}(\alpha,y)$, into the right-hand side to obtain the order-m-solution $G^{(m)}(\alpha,x)$. We assume that no IR-divergences appear. The integrand is finite because it is a power of a renormalized Green function, therefore the integral is only superficially divergent. The so-obtained divergence is of order α^m and can be absorbed by a suitable summand in $Z_G^{(m)}$, producing a finite $G^{(m)}(\alpha,x)$.

2.3. MOM scheme

The counterterms introduced in equation (2.3) are not unique. To fix them, one needs a renormalization condition. In the MOM scheme, this is done by fixing one particular momentum $\delta\cdot\mu^2$, where $\delta\in\mathbb{R}$ and μ is an arbitrary but fixed reference momentum.

One then demands the renormalized Green function to take the value unity at that momentum. Introducing $x := p^2/(\delta\mu^2)$, the MOM renormalization condition is

$$G(\alpha, x = 1) = 1 \quad \text{(MOM scheme)}. \tag{2.12}$$

This is achieved order by order in equation (2.11) if one includes not only the pole term (in ε), but all finite parts of the amplitude into the counterterm $Z^{(m)} = Z^{(m-1)} - \mathcal{R}[\ldots]$. The MOM-scheme operator $\mathcal{R}$ projects the integral to a fixed scale $x = 1$.

Using equation (2.10) and limits (2.9), the Callan–Symanzik equation (2.8) becomes

$$\gamma(\alpha)\Big(1 + s\alpha\frac{\partial}{\partial\alpha}\Big)G(\alpha, x) = x\frac{\partial}{\partial x}G(\alpha, x). \tag{2.13}$$

At the renormalization point $x = 1$, equations (2.13) and (2.12) lead to

$$\gamma(\alpha) = x\partial_x G(\alpha, x)|_{x=1}. \tag{2.14}$$

2.4. Expansion in logarithms

The renormalized solution of a 1-scale DSE in MOM-renormalization with renormalization point $x = 1$ can be expanded in logarithms according to

$$G(\alpha, x) = 1 + \sum_{k=1}^{\infty} \gamma_k(\alpha)(\ln x)^k. \tag{2.15}$$

From equation (2.14), we identify the anomalous dimension $\gamma_1(\alpha) = \gamma(\alpha)$. The functions $\gamma_{k>1}(\alpha)$ in equation (2.15), with invariant charge (2.2), can be computed from equation (2.13) [31]:

$$\gamma(\alpha)(1 + s\alpha\partial_\alpha)\gamma_{k-1}(\alpha) = k\gamma_k(\alpha). \tag{2.16}$$

In perturbation theory, all involved functions will be formal power series in α. In fact,

$$\gamma(\alpha) \in \mathcal{O}(\alpha), \quad \gamma_k(\alpha) \in \mathcal{O}(\alpha^k). \tag{2.17}$$

For a linear DSE, the exponent in the invariant charge (2.2) is $s = 0$, and consequently one obtains $\gamma_k(\alpha) = \frac{1}{k!}\gamma^k(\alpha)$. This corresponds to a scaling solution of equation (2.13),

$$G(\alpha, x) = x^{\gamma(\alpha)}. \tag{2.18}$$

The striking advantage of using MOM renormalization conditions for a Dyson–Schwinger equation is that the anomalous dimension $\gamma(\alpha)$ is the only truly unknown

function, and it itself can be computed from a non-linear ODE. This ODE is constructed by inserting the renormalization-group differential operator (2.16) into the Mellin transform of the primitive kernel [31, 44, 45]:

$$\frac{1}{-u \cdot M(u)}\Big|_{u\to -\gamma(1+s\alpha\partial_\alpha)}\gamma(\alpha) = \alpha. \tag{2.19}$$

See Appendix A for the Mellin transforms of the kernels used in this paper. A linear DSE with $s = 0$ reduces to the algebraic equation $M(-\gamma(\alpha)) = \alpha^{-1}$ [29].

There is a second expansion of the renormalized Green function $G(\alpha, x)$ in terms of logarithms, the leading log expansion. It is a reordering of equation (2.15) in powers of $(\alpha \ln x)$,

$$G(\alpha, x) = 1 + \sum_{k=1}^{\infty} H_k(\alpha \ln x)\alpha^k.$$

The function $H_1(z)$ is the leading log contribution to the Green function, and $H_k(z)$ represents the next-to^k leading log part. These expansions have been studied recently [20, 21, 32, 33], one of the results being that for a Dyson–Schwinger equation (2.11) with invariant charge (2.2), where $s \neq 0$ one has [32]

$$\begin{aligned}
H_1(z) &= (1 + sc_1 z)^{-\frac{1}{s}},\\
H_2(z) &= \frac{(1 + sc_1 z)^{-\frac{1}{s}-1}}{-sc_1} c_2 \ln(1 + sc_1 z),\\
H_3(z) &= \frac{(1 + sc_1 z)^{-\frac{1}{s}-2}}{s^2 c_1^2}\\
&\quad \times \left(s^2 c_1 z(c_2^2 - c_1 c_3) - sc_2^2 \ln(1 + sc_1 z) + \frac{c_2^2}{2}(1 + s)\ln^2(1 + sc_1 z)\right).
\end{aligned} \tag{2.20}$$

Here, $c_j = -[\alpha^j]\gamma(\alpha)$ is the j-th coefficient of the anomalous dimension. These general results will subsequently be used to cross-check our calculation.

2.5. Minimal subtraction scheme

In the minimal subtraction (MS) scheme, the counterterm $\hat{Z}^{(m)}$ is chosen to contain only the pole terms in ε, extracted by the operator $\hat{\mathcal{R}}$, of the integral at order m:

$$\hat{Z}^{(m)}(\varepsilon) = \hat{Z}^{(m-1)}(\varepsilon) - \left[\alpha \int \mathrm{d}y\, K(x, y) Q(G^{(m-1)})G^{(m-1)}\right] \quad \text{(MS scheme)}.$$

In MS, the anomalous dimension $\hat{\gamma}(\alpha)$ and the beta function $\hat{\beta}(\alpha)$ are again defined as derivatives of the $\hat{Z}$-factors, equations (2.5) and (2.6). This implies, using

equation (2.7), that they do not depend on ε at all: $\widehat{\beta}(\alpha,\varepsilon) = \widehat{\beta}(\alpha)$ and $\widehat{\gamma}(\alpha,\varepsilon) = \widehat{\gamma}(\alpha)$. Further, identity (2.10), $\widehat{\beta}(\alpha) = s\widehat{\gamma}(\alpha)$, still holds if $\widehat{Q} = \widehat{G}^s$. The so-defined renormalization group functions fulfil once more the Callan–Symanzik equation (2.8) and its limit for $\varepsilon \to 0$, equation (2.13). Note that for any given Feynman graph, the highest order pole in MS coincides with the one in MOM [28, Section 4], which is also clear from an induction over the coradical degree of the graph.

The fact that the counterterm in MS consists only of pole terms implies that the residues are closely related to the functions $\gamma_j(\alpha)$ in the log expansion (2.15). They satisfy a recursion very similar to equation (2.16), namely [18,30] and [19, Section 7]

$$\begin{aligned} \widehat{Z}_\alpha(\alpha,\varepsilon) &=: 1 + \sum_{j=1}^{\infty} \frac{1}{\varepsilon^j} \widehat{Z}_j(\alpha), \\ s\overline{\gamma}(\alpha) &= \overline{\beta}(\alpha) = \alpha\partial_\alpha Z_1(\alpha), \\ \alpha\partial_\alpha Z_j(\alpha) &= \beta\partial_\alpha(\alpha Z_{j-1}(\alpha)), \quad j > 1. \end{aligned} \tag{2.21}$$

The MS-bar renormalization scheme is a variant of MS where those finite terms which arise from a series expansion of $\frac{e^{\gamma_E}}{4\pi}$ are also subtracted. All quantities computed in minimal subtraction are denoted with a hat, like $\widehat{G}$. We denote MS-bar quantities with a bar, like $\overline{G}$. The undecorated quantities, like G, are in the MOM-scheme.

The MS-scheme involves a scale μ in the definition of $x = p^2/\mu^2$, but no explicit condition on the Green function is imposed. Intuitively, the MS-renormalized Green function $\widehat{G}(\alpha, x)$ will be unity at some other scale $p^2 = \widehat{\mu}^2 = \delta(\alpha)\cdot\mu^2$, where the factor $\delta(\alpha)$ is itself a function of α. One can view $\delta(\alpha)$ as the renormalization point to be chosen in MOM in order to reproduce the MS Green function. More mathematically, it was shown in [30, 38] that in the Hopf algebra formulation of perturbative quantum field theory, MS and MOM are equivalent up to a scaling of the renormalization point. The objective of the present work is to explicitly find this scaling $\delta(\alpha)$ for various Dyson–Schwinger equations.

3. Minimal subtraction scheme as a shifted MOM scheme

3.1. Shifted MOM renormalization point

The formulas of Section 2.4 are valid for MOM renormalization at $x = 1$. Now choose a kinematic renormalization point $\delta^{-1} \neq 1$. This is equivalent to choosing a reference momentum $\mu' = \sqrt{\delta}\cdot\mu$ instead of μ and using a new variable $x' := p^2/\mu'^2 = \delta^{-1}\cdot x$ such that $x = 1$ equals $x' = \delta^{-1}$. This setup is shown in Figure 1. The Green function $G'(x')$ is defined by

$$G(\alpha, x) = G(\alpha, \delta\cdot x') =: G'(\alpha, x') = G'(\alpha, \delta^{-1}\cdot x). \tag{3.1}$$

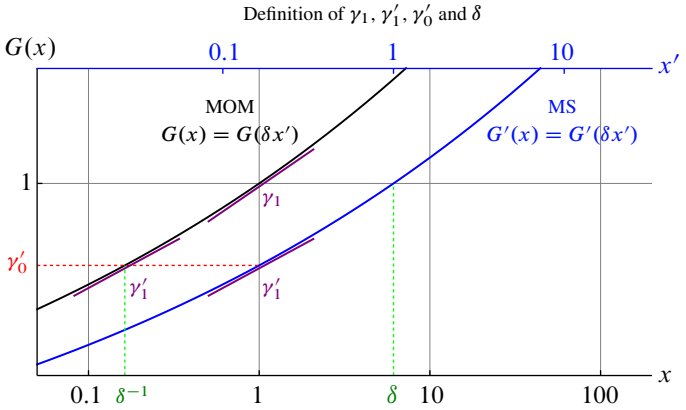

Figure 1. A hypothetical Green function in MOM ($G(x)$, black) and MS ($G'(x)$, blue). Both are initially given as functions of x (lower horizontal axis). We define a rescaled variable $x' = x \cdot \delta^{-1}$ such that $G'(x') = G(x)$. This means that $x = \delta$ (indicated in green) is the would-be kinematic renormalization point $x' = 1$. Conversely, γ_0' is the value $G'(x = 1)$ (red). This equals $G(x = \delta^{-1})$. The derivative γ_1 of $G(x)$ at $x = 1$ (purple) is different from the MS-derivative γ_1' at $x = 1$, which in turn equals the derivative of $G(x)$ at $x = \delta^{-1}$. It is $\gamma = \gamma_1$, but the new anomalous dimension γ' does not have a graphical representation in this plot since it is not defined as a simple derivative of G' with respect to x or x', see equation (2.6).

It has a log-expansion (in the original variable x, not x') similar to equation (2.15),

$$G'(x) = \gamma_0'(\alpha) + \sum_{k=1}^{\infty} \gamma_k'(\alpha)(\ln x)^k, \quad \gamma_k' = \sum_{j=k}^{\infty} \binom{j}{k} \gamma_j (\ln \delta)^{j-k}. \tag{3.2}$$

The first two of the new coefficients are, explicitly,

$$\begin{aligned} \gamma_0'(\alpha) &= G'(\alpha, 1) = G(\alpha, \delta^{-1}), \\ \gamma_1'(\alpha) &= x\partial_x G'(\alpha, x)\big|_{x=1} = x\partial_x G(\alpha, x)\big|_{x=\delta^{-1}}. \end{aligned} \tag{3.3}$$

Assume that $\ln(\delta)$ is a power series in α without pole terms. Therefore, the shifted functions $\gamma_k'(\alpha)$ start with the same coefficients as $\gamma_k(\alpha)$, using (2.17) we have

$$\gamma_k'(\alpha) \in \mathcal{O}(\alpha^k), \quad \gamma_k'(\alpha) = \gamma_k(\alpha) + \mathcal{O}(\alpha^{k+1}).$$

This means that the leading log function $H_1(z)$ (2.20) coincides.

Lemma 3.1. *Assume that the expansion functions $\gamma_k(\alpha)$ from equation (2.15) are formal power series and satisfy the Callan–Symanzik equation (2.16), and the kinematic renormalization point is shifted by a factor $\delta(\alpha)$ according to equation (3.1), which is a power series in α as well. Then:*

(1) *The new expansion functions $\gamma'_k(\alpha)$ are given by equation (3.2) and they again fulfil a Callan–Symanzik equation, but with the new anomalous dimension and beta function*

$$\gamma'(\alpha) := \frac{\gamma(\alpha)}{1 + s\gamma(\alpha) \cdot \alpha\partial_\alpha \ln \delta(\alpha)}, \quad \beta'(\alpha) := s\gamma'(\alpha). \tag{3.4}$$

(2) *The shifted anomalous dimension satisfies $\gamma'(\alpha) = \gamma(\alpha) + \mathcal{O}(\alpha^3)$.*

Proof. (1) The series representation of $\gamma'_k(\alpha)$ in equation (3.2) follows algebraically from expanding $\ln(x \cdot \delta(\alpha)) = \ln x + \ln \delta(\alpha)$ in the original log expansion (2.15). Compute the derivative of this series, using the fact that $\gamma_j(\alpha)$ satisfy equation (2.16), and identify the resulting series to obtain

$$\begin{aligned}
\alpha\partial_\alpha \gamma'_k(\alpha) = -\frac{\gamma}{s\gamma}\gamma'_k + \frac{1}{s\gamma} \sum_{j=k+1}^{\infty} \frac{j!(k+1)\gamma_j (\ln \delta)^{j-1-k}}{(j-1-k)!(k+1)!} \\
+ \alpha\partial_\alpha \ln \delta \cdot \sum_{j=k}^{\infty} \frac{j!(k+1)\gamma_j (\ln \delta)^{j-k-1}}{(j-k-1)!(k+1)!}, \\
(k+1)\gamma'_{k+1} = \frac{\gamma}{1 + s\gamma\alpha\partial_\alpha \ln \delta} \cdot \gamma'_k + \frac{s\gamma}{1 + s\gamma\alpha\partial_\alpha \ln \delta} \cdot \alpha\partial_\alpha \gamma'_k.
\end{aligned}$$

This is again the Callan–Symanzik equation, but with a different anomalous dimension and beta function as claimed in equation (3.4).

(2) Follows from equations (2.17) and (3.4) upon noting that

$$\gamma(\alpha) \cdot \alpha\partial_\alpha \ln \delta(\alpha) \in \mathcal{O}(\alpha^2). \qquad \blacksquare$$

We observe from equation (3.4) that for a linear DSE ($s = 0$), the anomalous dimensions in MS and MOM agree. On an algebraic level, this was remarked in [38, Example 5.12].

Note further that, if $\delta(\alpha)$ depends on α, the anomalous dimension $\gamma'(\alpha)$ of the shifted solution is not equal to $\gamma'_1(\alpha)$, the first derivative of the Green function (3.3). These two functions coincide only in the case of a kinematic renormalization scheme with a fixed (α-independent) renormalization point. If $\delta(\alpha)$ depends on α and $s \neq 0$ then there are two distinct effects happening at the same time: First, $\gamma'_1(\alpha) \neq \gamma_1(\alpha)$ because these derivatives are taken at different points, see Figure 1, and second, $\gamma'(\alpha) \neq \gamma(\alpha)$ because the moving renormalization point influences the Callan–Symanzik equation and definition (2.6).

In the remainder of the paper, we will be concerned with a reverse situation to Lemma 3.1. We are given two sets of functions, $\{\gamma_j\}$ and $\{\gamma'_j\}$, for example by expanding two known Green functions according to equation (2.15), and want to find $\delta(\alpha)$. We will mostly consider cases where both $\{\gamma_j\}$ and $\{\gamma'_j\}$ are solutions of the same

Dyson–Schwinger equation and hence both fulfil a Callan–Symanzik equation (2.16). But generally, the CSE is neither necessary nor sufficient for $\delta(\alpha)$ to exist. For example, let $\gamma_k(\alpha) = k\alpha^k$ and $\gamma'_k(\alpha) = \alpha^k(\alpha^2 + k)(1 - \alpha^2)^{-2-k}$, then neither γ_j nor γ'_j fulfil a CSE but they are related according to equation (3.2) with $\ln \delta(\alpha) = \alpha$. Conversely, the *chain approximation* is an example where the CSE is not satisfied and $\delta(\alpha)$ does not exist, see Section 7. Finally, two solutions of *different* Dyson–Schwinger equations do both fulfil a CSE and still they are in general not related by a $\delta(\alpha)$ as they fail to satisfy Lemma 3.1 (2).

3.2. Linear case

The goal of this paper is to determine the shift $\delta(\alpha)$ between kinematic renormalization (with a fixed renormalization point $x = 1$) and MS-renormalization. If we were to know the exact MS-solution $\widehat{G}(\alpha, \hat{x})$, then this amounts to finding the point $\hat{x} = \delta^{-1}(\alpha)$, where $\widehat{G}(\alpha, \delta^{-1}) = 1$.

Lemma 3.2. *Let $G(\alpha, x)$ and $G'(\alpha, x)$ be perturbative solutions of linear Dyson–Schwinger equations ($s = 0$ in both cases) with equal anomalous dimensions $\gamma(\alpha) = \gamma'(\alpha)$. Assume that $\gamma_0(\alpha), \gamma'_0(\alpha) = 1 + \mathcal{O}(\alpha)$ are formal power series starting with unity. Then the Green functions coincide in the sense of equation (3.1) if one chooses the α-dependent renormalization point given by the power series*

$$\ln \delta(\alpha) = \frac{1}{\gamma(\alpha)} \ln \frac{\gamma'_0(\alpha)}{\gamma_0(\alpha)}. \tag{3.5}$$

Proof. By Lemma 3.1 for $s = 0$, a necessary condition for a shift $\delta(\alpha)$ to exist is that the two Green functions must have the same anomalous dimension, which is guaranteed by assumption. It remains to show the reverse, that given the sets of functions $\{\gamma_j\}$ and $\{\gamma'_j\}$, it is always possible to find $\delta(\alpha)$.

In the linear case, $s = 0$, the solution of the Callan–Symanzik equation (2.13) is a monomial $G(\alpha, x) = \gamma_0(\alpha)x^{\gamma(\alpha)}$. Using equation (3.1), we demand $\gamma'_0 = \gamma_0\delta^\gamma$, which leads to the claimed formula. The functions $\gamma(\alpha)$, $\gamma_0(\alpha)$ and $\gamma'_0(\alpha)$ are power series and $\gamma'_0(\alpha)/\gamma(\alpha) = 1 + \mathcal{O}(\alpha)$ by assumption. Therefore, $\ln(\gamma'_0/\gamma_0) \in \mathcal{O}(\alpha)$ and the pole $1/\alpha$ of $1/\gamma(\alpha)$ from equation (2.17) is cancelled. The right-hand side of equation (3.5) is a formal power series indeed. ∎

In MOM, we have $\gamma_0(\alpha) = 1$ by the renormalization condition (2.12), and hence equation (2.18). In MS, the solution will have some $\widehat{\gamma}_0(\alpha) \neq 1$, which is the value of $G'(\alpha, 1)$, see equation (3.3). Lemma 3.2 thus specializes to

$$\ln \delta(\alpha) = \frac{\ln \widehat{\gamma}_0}{\gamma(\alpha)}. \tag{3.6}$$

It is also possible to infer $\hat{\gamma}_0(\alpha)$ from the MOM-solution alone. To this end, note that the MS Green function is proportional to the one in MOM. Going back to definition (2.3) of the Z-factors, this means that $\hat{Z}G_0 = \hat{\gamma}_0 \cdot ZG_0 + \mathcal{O}(\varepsilon)$. From the integral representations (2.7), using that in MS $\hat{\gamma}(\alpha, \varepsilon) = \hat{\gamma}(\alpha)$, we get

$$\begin{aligned} e^{-\int_0^\alpha \frac{\mathrm{d}u}{u} \frac{\hat{\gamma}(u)}{\varepsilon}} &= \hat{\gamma}_0(\alpha) \cdot e^{-\int_0^\alpha \frac{\mathrm{d}u}{u} \frac{\gamma(u,\varepsilon)}{\varepsilon}} + \mathcal{O}(\varepsilon) \\ &\Rightarrow \gamma(\alpha, \varepsilon) = \gamma(\alpha) - \varepsilon\alpha\partial_\alpha \ln \hat{\gamma}_0(\alpha) + \mathcal{O}(\varepsilon^2). \end{aligned}$$

If we know the MOM anomalous dimension for $\varepsilon \neq 0$, then we can compute $\hat{\gamma}_0$ and hence $\ln \delta$ from

$$\alpha\partial_\alpha \ln \hat{\gamma}_0(\alpha) = -[\varepsilon^1]\gamma(\alpha, \varepsilon). \tag{3.7}$$

In fact, for a linear DSE all coefficients of the MOM counterterm $Z(\alpha, \varepsilon)$ are directly given by the ε-expansion of the MOM anomalous dimension via equation (2.7):

$$\begin{aligned} Z(\alpha, \varepsilon) &=: \exp\Big(-\sum_{n=-1}^{\infty} \varepsilon^n \cdot z_n(\alpha)\Big), \\ \alpha\partial_\alpha z_n(\alpha) &= [\varepsilon^{n+1}]\gamma(\alpha, \varepsilon), \quad z_0(\alpha) = \ln \hat{\gamma}_0(\alpha). \end{aligned} \tag{3.8}$$

For the counterterm $\hat{Z}(\alpha, \varepsilon)$ in MS, all $\hat{z}_{n\geq 0}(\alpha)$ vanish, as do the ε-dependent parts of $\hat{\gamma}(\alpha, \varepsilon) = \hat{\gamma}(\alpha)$.

3.3. Non-linear case

Lemma 3.3. *Assume $\gamma_k(\alpha)$ and $\gamma(\alpha)$ are the expansion coefficients respectively the anomalous dimension in kinematic renormalization, and $\gamma'_k(\alpha)$, $\gamma'(\alpha)$ the corresponding quantities in MS, of the perturbative solution of the same Dyson–Schwinger equation of type (2.11). Then the first two orders of the anomalous dimensions coincide, $\gamma'(\alpha) = \gamma(\alpha) + \mathcal{O}(\alpha^3)$.*

Proof. Let $f_n^{(k)}$ be the coefficients of the ε-expansion of the kernel graph according to Appendix B. Then the first coefficients of an explicit perturbative solution of equation (2.11) in MOM and MS are

$$\begin{aligned} \gamma(\alpha) &= -f_{-1}^{(0)}\alpha + (s+1)(-2f_{-1}^{(0)}f_0^{(1)} - 2f_0^{(0)}f_{-1}^{(1)} + 2f_{-1}^{(0)}f_0^{(0)})\alpha^2 + \mathcal{O}(\alpha^3), \\ \hat{\gamma}_1(\alpha) &= -f_{-1}^{(0)}\alpha + (s+1)(-2f_{-1}^{(0)}f_0^{(1)} - 2f_0^{(0)}f_{-1}^{(1)} + f_{-1}^{(0)}f_0^{(0)})\alpha^2 + \mathcal{O}(\alpha^3), \\ \hat{\gamma}_0(\alpha) &= 1 + \alpha f_0^{(0)} + \mathcal{O}(\alpha^2), \quad \alpha\partial_\alpha \hat{G}|_{x=1} = \alpha f_0^{(0)} + \mathcal{O}(\alpha^2). \end{aligned}$$

Using the Callan–Symanzik equation (2.8) and formulas (3.3), the anomalous dimension in MS is

$$\widehat{\gamma}(\alpha) = \frac{\widehat{\gamma}_1(\alpha)}{\widehat{\gamma}_0(\alpha) + s\alpha\partial_\alpha \widehat{G}|_{x=1}} = \frac{\widehat{\gamma}_1(\alpha)}{1 + (s+1)\alpha f_0^{(0)} + \mathcal{O}(\alpha^2)} = \gamma(\alpha) + \mathcal{O}(\alpha^3). \quad \blacksquare$$

We now assume that we know the MOM- and the MS-solution and their corresponding counterterms, and hence the renormalization group functions, by explicit calculation. The remaining task is then to extract the shift $\delta(\alpha)$ from this data.

The constant coefficient of the power series $\ln \delta(\alpha)$ can be inferred from equation (3.2), $\widehat{\gamma}_0 = 1 + \gamma_1 \ln \delta + \mathcal{O}(\alpha^2)$. We insert the series from the proof of Lemma 3.3 and read off

$$\ln \delta(\alpha) = -f_0^{(0)}(f_{-1}^{(0)})^{-1} + \mathcal{O}(\alpha). \tag{3.9}$$

Note that $f_{-1}^{(0)} \neq 0$ in physically sensible kernels. Remarkably, $\delta(0) = e^{-f_0^{(0)}/f_{-1}^{(0)}} \neq 1$ unless $f_0^{(0)} = 0$, so the shift does not necessarily vanish for vanishing coupling. This result does not depend on the invariant charge in the DSE, or whether it is linear or non-linear, but just on the primitive kernel.

Theorem 3.4. *Let $G(\alpha, x)$ and $\widehat{G}(\alpha, x)$ be the perturbative solutions of the same propagator-type Dyson–Schwinger equation (2.11), where G uses kinematic renormalization and $\widehat{G}$ minimal subtraction. Assume that $\gamma(\alpha)$, $\widehat{\gamma}(\alpha)$ are power series with a non-vanishing term $\propto \alpha$. Then there is a unique power series $\delta(\alpha)$ such that $G(\alpha, \delta(\alpha)\cdot x) = \widehat{G}(\alpha, x)$ for all x, given by equation (3.9) and*

$$\frac{\partial}{\partial\alpha} \ln \delta(\alpha) = \frac{1}{s\alpha}\Big(\frac{1}{\widehat{\gamma}(\alpha)} - \frac{1}{\gamma(\alpha)}\Big) = \frac{\gamma(\alpha) - \widehat{\gamma}(\alpha)}{s\alpha\widehat{\gamma}(\alpha)\gamma(\alpha)}. \tag{3.10}$$

Proof. The function $\delta(\alpha)$ for the linear case $s = 0$ was constructed explicitly in Lemma (3.2). It remains to consider $s \neq 0$.

The fact that MS and MOM are related via a change in renormalization point, or equivalently, via a change in the value of the renormalized coupling, is known from a Hopf-algebraic analysis, see [28, 30, 38]. It remains to show that, in our setup, the shift $\delta(\alpha)$ is a well-defined power series.

From Lemma 3.1, we know how shifting the kinematic renormalization point induces a change in the anomalous dimension. Solving equation (3.4) for $\delta(\alpha)$ produces equation (3.10).

By equations (2.17) and (3.4) and assumption, the denominator of the last fraction is proportional to α^3. But, since $\widehat{\gamma}(\alpha)$ is the anomalous dimension in MS, the numerator is $\gamma(\alpha) - \widehat{\gamma}(\alpha) \in \mathcal{O}(\alpha^3)$ by Lemma 3.3. Therefore, the right-hand side of equation (3.10) is a well-defined power series in α. It uniquely defines the power series $\delta(\alpha)$ up to a constant summand, which is fixed by equation (3.9).

Since we know that MS and MOM are related via a shifted renormalization point, the so-constructed shift $\delta(\alpha)$ necessarily also gives rise to the correct $\widehat{\gamma}_0(\alpha)$, uniquely defined via

$$\widehat{\gamma}_0(\alpha) = \sum_{j=0}^{\infty} \gamma_j(\alpha)(\ln \delta(\alpha))^j .$$

By assumption, the Green function $\widehat{G}(\alpha, x)$ satisfies the Callan–Symanzik equation with anomalous dimension $\widehat{\gamma}(\alpha)$, hence by Lemma 3.1 from $\widehat{\gamma}_0(\alpha)$ also all other functions $\widehat{\gamma}_j(\alpha)$ are reproduced correctly. ∎

Given the solutions of a DSE in MOM and MS, there are at least three approaches to calculate $\delta(\alpha)$ from this data. The first approach directly uses equation (3.10), where the anomalous dimensions $\gamma(\alpha)$, $\widehat{\gamma}(\alpha)$ can be extracted from the corresponding Z-factors with the help of equations (2.7) and (2.21).

The second approach utilizes the renormalization group equation in MS derived in Lemma 3.1,

$$(k+1)\widehat{\gamma}_{k+1}(\alpha) = \frac{\gamma(\alpha)}{1 + s\gamma(\alpha)\alpha\partial_\alpha \ln \delta(\alpha)} \cdot (1 + s\alpha\partial_\alpha)\widehat{\gamma}_k(\alpha). \tag{3.11}$$

If any two of the MS functions $\widehat{\gamma}_k(\alpha)$, together with the MOM anomalous dimension $\gamma(\alpha)$, are known, then $\delta(\alpha)$ can be computed. For example, using $\widehat{\gamma}_0$ and $\widehat{\gamma}_1$, one has

$$\frac{\partial}{\partial\alpha} \ln \delta(\alpha) = \frac{\gamma \cdot \widehat{\gamma}_0 - \widehat{\gamma}_1}{s\alpha \cdot \widehat{\gamma}_1} + \frac{1}{\widehat{\gamma}_1} \frac{\partial}{\partial\alpha} \widehat{\gamma}_0 \qquad \text{for } s \neq 0.$$

The third, and computationally most efficient, approach is to compute all MS functions $\widehat{\gamma}_j(\alpha)$ up to some desired maximum j and additionally all MOM functions $\gamma_j(\alpha)$. Next, one writes a power series ansatz for $\ln \delta(\alpha)$ and uses this to formally compute the powers $(\ln \delta(\alpha))^k$. Then the right-hand side of equation (3.2) is a linear system for the unknown coefficients of $\ln \delta(\alpha)$ which can be solved.

All three approaches are different ways to solve the same equations, therefore the resulting $\ln \delta(\alpha)$ agree. The third approach does not involve a derivative and therefore it produces one order higher in α compared to the first two, for the same order of input data.

We want to stress that, despite the above considerations, it is in general not possible to recover the MS Green function from the MOM one or vice versa when only the limit $\varepsilon \to 0$ is known. The shift $\delta(\alpha)$ is a truly unknown function which depends on the particular DSE and on the integral kernel. In the remainder of the paper, we will explicitly compute $\delta(\alpha)$ for three different Dyson–Schwinger equations.

4. Linear Dyson–Schwinger equation in $D = 4 - 2\varepsilon$ dimensions

We first consider a linear Dyson–Schwinger equation of iterated one-loop Feynman graphs, namely

$$\widehat{G}(q^2) = 1 + \lambda \int \frac{\mathrm{d}^D k}{(2\pi)^D} \frac{\widehat{G}(k^2)}{(k+q)^2 k^2} - \widehat{\mathcal{R}}\Big[\lambda \int \frac{\mathrm{d}^D k}{(2\pi)^D} \frac{\widehat{G}(k^2)}{(k+q)^2 k^2}\Big]. \tag{4.1}$$

Here, λ is a coupling constant and $D = 4 - 2\varepsilon$ is the spacetime dimension. Equation (4.1) is the linear DSE (rainbow approximation) for the fermion propagator in Yukawa theory, but scaled and projected onto suitable tensors such that the order zero (tree level) solution is

$$\widehat{G}^{(0)}(q^2) := 1. \tag{4.2}$$

4.1. Computation of the coefficients

One can solve the DSE (4.1) to first order by inserting equation (4.2) into it and computing the integrals according to Appendix B:

$$\widehat{G}^{(1)}(q^2) = 1 + \frac{\lambda}{(4\pi)^2}(1 - \widehat{\mathcal{R}})\Big[(4\pi)^{\varepsilon} e^{-\gamma_E \varepsilon} \Big(\frac{q^2}{m^2}\Big)^{-\varepsilon} \sum_{w=-1}^{\infty} f_w^{(0)} \varepsilon^w\Big]. \tag{4.3}$$

Here, m^2 is an arbitrary mass scale introduced for dimensional reasons and the coefficients $f_w^{(k)}$ are given in equation (B.2). The operator $\widehat{\mathcal{R}}$ projects the pole part of this equation, which is $f_{-1}^{(0)} \varepsilon^{-1}$. This pole part is independent of momenta as expected in a locally renormalizable theory.

For a systematic treatment of higher orders, it will be advantageous to include the counterterm as a summand $\propto 1 = (q^2)^0$ into the solution. Define

$$\overline{g}_{1,w}^{(1)} := f_w^{(0)}, \quad \overline{g}_{0,w}^{(1)} := \begin{cases} -f_{-1}^{(0)} & \text{if } w = -1, \\ 0 & \text{else,} \end{cases}$$

then the renormalized solution to order one, equation (4.3), is

$$\widehat{G}^{(1)}(q^2) = 1 + \frac{\lambda}{(4\pi)^2} \sum_{t=0}^{1} (4\pi)^{t\varepsilon} e^{-\gamma_E t\varepsilon} \Big(\frac{q^2}{m^2}\Big)^{-t\varepsilon} \sum_{w=-1}^{\infty} \overline{g}_{t,w}^{(1)} \varepsilon^w. \tag{4.4}$$

The factor $(4\pi)^{t\varepsilon} e^{-\gamma_E t\varepsilon}$ eventually produces finite contributions $\propto \gamma_E$ and $\propto \ln(4\pi)$. In MS renormalization, these terms are present in the finite part of $\widehat{G}$ while in MS-bar renormalization they are assigned to the counterterm $\overline{Z}$ and thus absent from $\overline{G}$. To facilitate computations, we will absorb them into the momentum variable. This

way, we effectively obtain the MS-bar Green function of the new momentum variable. On the other hand, our counterterm will be $\widehat{Z}$ in MS as it does not contain the $\ln(4\pi)$, γ_E contributions either. This way, we can skip in every intermediate step two additional series expansions, the ones of $e^{-\gamma_E t\varepsilon}$ and $e^{\ln(4\pi)t\varepsilon}$. Let therefore

$$\hat{x} := \frac{q^2}{m^2}, \quad \bar{x} := \frac{e^{\gamma_E} q^2}{4\pi m^2} \equiv \frac{q^2}{\bar{m}^2}, \quad \hat{G}(\hat{x}) \equiv \bar{G}(\bar{x}). \tag{4.5}$$

The transition $\hat{x} \leftrightarrow \bar{x}$ is a rescaling of the momentum which can also be understood as choosing a suitable value of the reference momentum m, as evidenced by the second equal sign where $\bar{m}^2 = 4\pi e^{-\gamma_E} m^2$. This is not kinematic renormalization: m is merely the unit used for the momenta, the MS-renormalized Green function $\hat{G}(q^2)$ does not fulfil any particular condition at the point $q^2 = m^2$. Also, m^2 is not the mass of a particle, the field is still massless. Finally, let $\alpha := \lambda(4\pi)^{-2}$.

Higher orders of the renormalized Green function are computed iteratively. Assume that we know the solution to order $(m-1)$,

$$\bar{G}^{(m-1)}(\alpha, \bar{x}) = \bar{G}^{(m-2)}(\alpha, \bar{x}) + \alpha^{m-1} \sum_{t=0}^{m-1} (\bar{x})^{-t\varepsilon} \sum_{w=-(m-1)}^{\infty} \bar{g}_{t,w}^{(m-1)} \varepsilon^w .$$

Inserting this into equation (4.1), the order m solution is

$$\bar{G}^{(m)}(\alpha, \bar{x}) = \bar{G}^{(m-1)}(\alpha, \bar{x}) + \alpha^{m} \sum_{t=0}^{m} (\bar{x})^{-t\varepsilon} \sum_{w=-m}^{\infty} \bar{g}_{t,w}^{(m)} \varepsilon^w , \tag{4.6}$$

where the new coefficients are determined by

$$\bar{g}_{u,w}^{(m)} := \sum_{n=-m+1}^{w+1} \bar{g}_{u-1,n}^{(m-1)} f_{w-n}^{(u-1)} \quad \forall u > 0. \tag{4.7}$$

The counterterm is included in this sum as the $t = 0$ summand. The coefficient of order ε^w in the MS-counterterm at m loops is

$$\bar{g}_{0,w}^{(m)} = \begin{cases} -\sum_{u=1}^{m} \bar{g}_{u,w}^{(m)} & \text{if } w \in \{-m, \dots, -1\}, \\ 0 & \text{else.} \end{cases} \tag{4.8}$$

The all-order perturbative solution $\bar{G}(\bar{x})$ of equation (4.1) is defined as the limit $m \to \infty$ in equation (4.6), effectively it is an infinite sum over the orders α^m in the coupling. We exchange the sums to expose expansion (2.15) and the counterterm $\widehat{Z}$:

$$\bar{G}(\alpha, \bar{x}) = \widehat{Z}(\alpha, \varepsilon) + \sum_{k=0}^{\infty} \ln(\bar{x})^k \sum_{t=1}^{\infty} \frac{(-t)^k}{k!} \sum_{m=t}^{\infty} \alpha^m \sum_{w=-m}^{\infty} \bar{g}_{t,w}^{(m)} \varepsilon^{k+w}. \tag{4.9}$$

As explained above (4.5), we have introduced the MS (not MS-bar) counterterm,

$$\hat{Z}(\alpha,\varepsilon) := 1 + \sum_{m=1}^{\infty} \alpha^m \sum_{w=-m}^{-1} \bar{g}^{(m)}_{0,w} \varepsilon^w = 1 - \sum_{m=1}^{\infty} \alpha^m \sum_{w=-m}^{-1} \sum_{t=1}^{m} \bar{g}^{(m)}_{t,w} \varepsilon^w. \quad (4.10)$$

Equations (4.9) and (4.10) together with the recursion relations (4.7) and (4.8) allow us to compute the solution of the DSE (4.1) to arbitrary order.

A similar procedure can be used to obtain the MOM-renormalized finite Green function $G(\bar{x})$. One merely has to extend equation (4.7) to include all orders w of ε. If we are only interested in the finite (as $\varepsilon \to 0$) part, then, in a linear DSE, it is sufficient to include the $w = 0$ term into the counterterm. To this end, instead of equations (4.7) and (4.8) one uses

$$g^{(m)}_{u,w} := \begin{cases} \sum_{n=-m+1}^{w+1} g^{(m-1)}_{u-1,n} f^{(u-1)}_{w-n} & \text{if } u > 0, \\ -\sum_{u=1}^{m} g^{(m)}_{u,w} & \text{if } u = 0 \text{ and } w \in \{-m,\dots,0\}, \\ 0 & \text{else.} \end{cases} \quad (4.11)$$

We will call this prescription "pseudo-MOM-scheme", since the counterterm computed by equation (4.11) is not the true counterterm of kinematic renormalization, it misses higher orders in ε. But this prescription produces finite Green function

$$G(\alpha,\bar{x}) = Z(\alpha,\varepsilon) + \sum_{k=0}^{\infty} \ln(\bar{x})^k \frac{1}{k!} \sum_{m=1}^{\infty} \alpha^m \sum_{t=1}^{m} (-t)^k \sum_{w=-m}^{\infty} g^{(m)}_{t,w} \varepsilon^{k+w}, \quad (4.12)$$

which for $\varepsilon \to 0$ is conventionally MOM-renormalized. It by construction takes the value unity at the renormalization point $\bar{x} = 1$, i.e., at the momentum $q^2 = \mu^2$. Now the interpretation of μ^2 has changed: In the MS- or MS-bar-solutions, it was an arbitrary momentum scale without particular meaning for the Green function while in MOM it is the momentum where $G(\alpha, q^2/\mu^2) = 1$.

4.2. Renormalized correlation function

In MOM renormalization, the analytic solution of this linear DSE has long been known [23]. As always for a linear DSE, it is a pure scaling solution where the anomalous dimension $\gamma(\alpha)$ is determined from the Mellin transform of the primitive, see equation (2.19) and Appendix A. With the notation of equation (2.15), the MOM-solution at $\varepsilon = 0$ reads

$$G(\alpha,\bar{x}) = \bar{x}^{\gamma(\alpha)}, \quad (4.13)$$

where

$$\gamma_0(\alpha) = 1, \quad \gamma(\alpha) = \frac{\sqrt{1-4\alpha}-1}{2} = -\sum_{n=1}^{\infty} C_{n-1}\alpha^n, \quad \gamma_k(\alpha) = \frac{1}{k!}(\gamma(\alpha))^k.$$

Here, C_n are the Catalan numbers. It has been verified symbolically up to order α^{25} that the series in equation (4.12) indeed coincides with equation (4.13) in the limit $\varepsilon \to 0$.

In MS-bar-renormalization, there is a finite remainder term in the ε^0-coefficient of each order in α, which would have been subtracted in kinematic renormalization. Therefore, the MS-bar-coefficients $\overline{\gamma}_k(\alpha)$ in equation (2.15) are generally different from the MOM-coefficients $\gamma_k(\alpha)$, see Section 3.1. We compute $\delta(\alpha)$ from $\overline{\gamma}_0(\alpha)$ via equation (3.6). From equation (4.9), one reads off

$$\begin{aligned}\overline{\gamma}_0(\alpha) &= 1 + \sum_{m=1}^{\infty} \alpha^m \sum_{t=1}^{m} \overline{g}_{t,0}^{(m)} \\ &= 1 + 2\alpha + \frac{11}{2}\alpha^2 + \frac{51 - 2\zeta(3)}{3}\alpha^3 + \frac{1341 - 80\zeta(3)}{24}\alpha^4 + \mathcal{O}(\alpha^5). \end{aligned} \tag{4.14}$$

We have used that the $\widehat{Z}$-factor in MS has, at finite order, only terms singular in ε and therefore does not contribute to $\overline{\gamma}_k$, and the summand $t = 0$ can be left out. For the interpretation as a change of renormalization point, the remaining functions $\overline{\gamma}_k(\alpha)$ have to be consistent with equations (3.2) and (4.13). It has been verified to order α^{25} and for $k \leq 15$ that indeed $\overline{\gamma}_k(\alpha) = \overline{\gamma}_0(\alpha) \cdot \gamma_k(\alpha)$.

Remarkably, for the linear DSE (4.1) considered here, it is possible to find a closed formula for $\overline{\gamma}_0(\alpha)$. To do this, one computes the logarithm of the series (4.14) and repeatedly uses the OEIS [36]. One can first identify the rational coefficients and their generating function. Subtracting that part one is left with

$$\begin{aligned}&\ln \overline{\gamma}_0 - \ln\Big(\frac{1 - \sqrt{1-4\alpha}}{2\alpha(1-4\alpha)^{\frac{1}{4}}}\Big) \\ &\quad = -\zeta(3)\Big(2\frac{\alpha^3}{3} + 8\frac{\alpha^4}{4} + 30\frac{\alpha^5}{5} + 112\frac{\alpha^6}{6} + 420\frac{\alpha^7}{7} + 1584\frac{\alpha^8}{8} + \cdots\Big) \\ &\qquad - \zeta(5)\Big(2\frac{\alpha^5}{5} + 12\frac{\alpha^6}{6} + 56\frac{\alpha^7}{7} + 240\frac{\alpha^8}{8} + 990\frac{\alpha^9}{9} + \cdots\Big) - \zeta(7) - \cdots .\end{aligned}$$

At least up to $\zeta(11)$ and α^{25}, the coefficients of $(\alpha^{j+m-1})/(j+m-1)$ in the term proportional to $\zeta(m)$ are given by the binomial coefficient $2\binom{2j+m-3}{j-1}$. Assuming again that this holds universally, all series over α and then the remaining series in $\zeta(m)$ can be summed and yield known functions. The result is

$$\begin{aligned}\overline{\gamma}_0(\alpha) &= e^{\gamma_E(1-\sqrt{1-4\alpha})} \frac{1 - \sqrt{1-4\alpha}}{2\alpha(1-4\alpha)^{\frac{1}{4}}} \frac{\Gamma(\frac{3}{2} - \frac{1}{2}\sqrt{1-4\alpha})}{\Gamma(\frac{1}{2} + \frac{1}{2}\sqrt{1-4\alpha})} \\ &= \frac{-\gamma}{\alpha}\sqrt{\frac{\mathrm{d}\,(-\gamma)}{\mathrm{d}\alpha}} e^{-2\gamma\gamma_E} \frac{\Gamma(1-\gamma)}{\Gamma(1+\gamma)}. \end{aligned} \tag{4.15}$$

In the latter form, $\gamma \equiv \gamma(\alpha)$ is the anomalous dimension from equation (4.13). We remark that such fraction of Euler gamma functions is not uncommon in the computation of multiedge Feynman graphs, compare for example [7].

With this function $\overline{\gamma}_0(\alpha)$ and equation (4.13), the MS-bar-renormalized solution $\overline{G}(\overline{x})$ in the limit $\varepsilon \to 0$ reads explicitly

$$\overline{G}(\alpha, \overline{x}) = \overline{\gamma}_0(\alpha) \cdot G(\alpha, \overline{x}) = \overline{\gamma}_0(\alpha) \cdot \overline{x}^{\gamma(\alpha)}.$$

From equation (4.5), one can reconstruct the MS-renormalized function $\widehat{G}(\hat{p}^2)$:

$$\widehat{G}(\alpha, \hat{x}) = \overline{G}\Big(\alpha, \frac{\hat{x}}{4\pi e^{-\gamma_E}}\Big) = \widehat{\gamma}_0(\alpha) \cdot \hat{x}^{\gamma(\alpha)},$$

where $\widehat{\gamma}_0(\alpha) := (4\pi e^{-\gamma_E})^{-\gamma(\alpha)} \cdot \overline{\gamma}_0(\alpha)$.

Following Section 3.1, the correspondence between MS-, MS-bar- and MOM-renormalized Green functions can equivalently be expressed by their respective renormalization points. Let μ be the mass scale in MS- and MS-bar-renormalization. Then the Green function is unity at $x = \widehat{\delta}^{-1}$ and $x = \overline{\delta}^{-1}$, respectively. Equivalently, $\widehat{\mu}^2 = \widehat{\delta} \cdot \mu^2$ and $\overline{\mu}^2 = \overline{\delta} \cdot \mu^2$ are the mass scales one needs to choose for MS and MS-bar, in order to reproduce kinematic renormalization at the scale μ^2:

$$G\Big(\alpha, \frac{q^2}{\mu^2}\Big) \equiv \overline{G}\Big(\alpha, \frac{q^2}{\overline{\mu}^2}\Big) \equiv \widehat{G}\Big(\alpha, \frac{q^2}{\widehat{\mu}^2}\Big).$$

By equations (3.6), (4.15) and (4.13), these scales are related via

$$\begin{aligned}
\overline{\delta}(\alpha) &= \overline{\gamma}_0^{\frac{1}{\gamma}} = e^{-2}\Big(1 - \frac{3}{2}\alpha - \Big(\frac{49}{24} - \frac{2}{3}\zeta(3)\Big)\alpha^2 + \mathcal{O}(\alpha^3)\Big), \\
\widehat{\delta}(\alpha) &= \widehat{\gamma}_0^{\frac{1}{\gamma}} = \frac{\overline{\delta}(\alpha)}{\sqrt{4\pi e^{-\gamma_E}}}.
\end{aligned}$$

The latter of course reproduces the transformation $m \leftrightarrow \overline{m}$ in equation (4.5). The zeroth order coefficient is e^{-2} as expected from equation (3.9), where $f_{-1} = f_{-1}^{(0)} = 1$, $f_0 = f_0^{(0)} = 2$. In any case, the shift between renormalization schemes is a finite function as long as $\alpha < \frac{1}{4}$, shown in Figure 2.

4.3. Counterterm and ε-dependence

Our calculation (up to order α^{25}) delivers for the counterterm in MS the series coefficients

$$\ln(\widehat{Z}(\alpha, \varepsilon)) = -\frac{1}{\varepsilon}\Big(\alpha + \frac{\alpha^2}{2} + 2\frac{\alpha^3}{3} + 5\frac{\alpha^4}{4} + 14\frac{\alpha^5}{5} + 42\frac{\alpha^6}{6} + \cdots\Big).$$

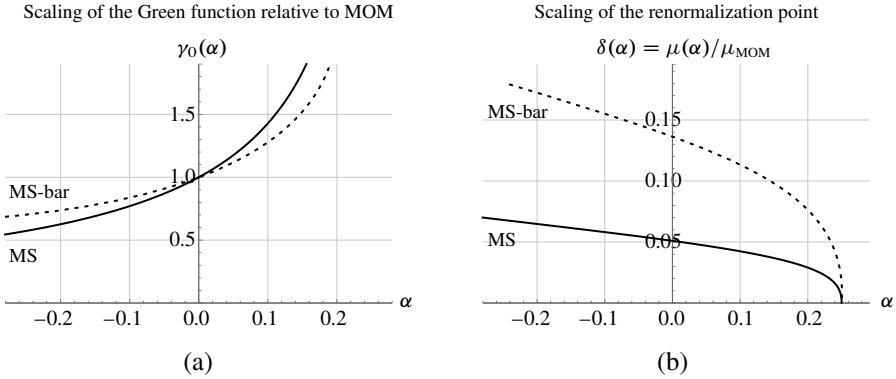

Figure 2. (a) Behaviour of the MS scaling-function $\widehat{\gamma}_0(\alpha)$ (thick) and the MS-bar scaling function $\overline{\gamma}_0(\alpha)$ (dashed) as functions of the renormalized coupling α. Both are unity at $\alpha = 0$ and diverge at $\alpha = 1/4$. (b) Rescaling factor $\delta(\alpha)$ according to Section 3.1 of the reference momentum in MS-renormalization $\widehat{\mu}$ (thick) and MS-bar-renormalization $\overline{\mu}$ (dashed) relative to the MOM-renormalization-point μ. The functions are equal up to the factor $\sqrt{4\pi e^{-\gamma_E}}$. They are not unity for $\alpha = 0$.

Once more we recognize the Catalan numbers and introduce $\gamma = \gamma(\alpha)$ from equation (4.13),

$$\begin{aligned}\widehat{Z}(\alpha,\varepsilon) &= \exp\left(-\frac{1}{\varepsilon}\sum_{m=1}^{\infty} C_{n-1}\frac{\alpha^n}{n}\right) = e^{-\frac{1}{\varepsilon}\left(1-\sqrt{1-4\alpha}+\ln\left(1-\frac{1-\sqrt{1-4\alpha}}{2}\right)\right)} \\ &= e^{\frac{1}{\varepsilon}(2\gamma-\ln(1+\gamma))}. \end{aligned} \tag{4.16}$$

This expression is the integral of $\gamma(\alpha)$, as expected from equation (2.7) for a linear DSE. As long as α and ε have the same sign, this function has the limit $\widehat{Z}(\alpha, 0^+) = 0$ when $\varepsilon \to 0$, see Figure 3. With equation (4.16), the counterterm turns out to be a remarkably well-behaved function of ε, compared to its perturbative expansion, where every single term diverges as $\varepsilon \to 0$. This is in line with [34] and a comment made in [29]: The all-order-solution (4.13) "regulates itself" by its anomalous dimension. The integral in the DSE (4.1) is not divergent and the remaining finite counterterm is set to zero in MOM by choice of the renormalization point. Figure 3 shows how $\widehat{Z}$ approaches zero as the scaling solution $\varepsilon = 0$ is reached.

Using expansion (3.8), it has been verified to order α^{20} that $z_{-1}(\alpha) = \overline{z}_{-1}(\alpha)$ is given by $\gamma(\alpha) = \overline{\gamma}(\alpha)$ and that the MOM-coefficient $z_0(\alpha)$ fulfils $z_0(\alpha) = \ln \overline{\gamma}_0(\alpha)$ as expected. In our simplified MOM-scheme (4.11), all other $z_{n>0}$ vanish. In true kinematic renormalization, they are present. The author computed the coefficients $z_{n\leq 9}$ up to order α^{10} but did not succeed in finding generating functions. However,

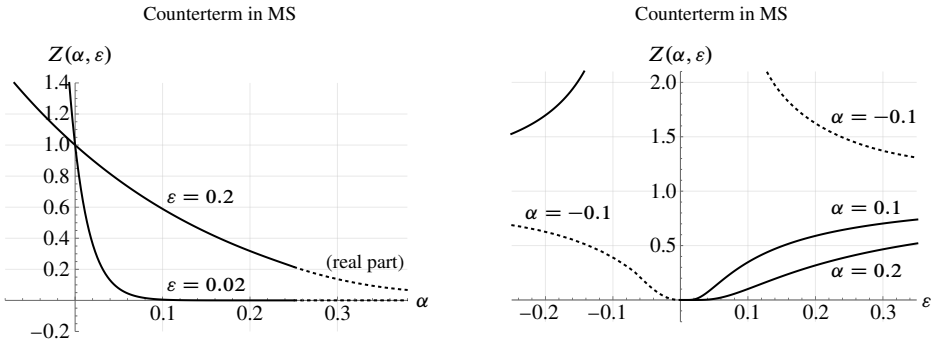

Figure 3. (a) Counterterm $\hat{Z}(\alpha, \varepsilon)$ in MS as a function of the renormalized coupling α for different values of ε. As $\varepsilon \to 0^+$, the function approaches zero for $\alpha > 0$ and diverges for $\alpha < 0$. For $\alpha > 1/4$, the counterterm acquires an imaginary part which is not shown. (b) The same counterterm as a function of ε for fixed values of α. For positive α, the counterterm smoothly approaches the value zero as $\varepsilon \to 0^+$.

it turned out that all $z_{n\leq 9}(\alpha)$ for $0 < \alpha < \frac{1}{4}$ are, within the computed order, strictly positive. This implies that the exponent is strictly negative for all $\varepsilon > 0$ and hence $Z(\alpha, \varepsilon) \in [0, 1]$. The classical interpretation of the Z-factor as a probability requires these bounds. Compare [26, Section 8] for the various interpretations of Z and their relations.

5. Linear Dyson–Schwinger equation in $D = 6 - 2\varepsilon$ dimensions

For the 6-dimensional case, the procedure is completely analogous to the one described in the previous section. We will use the same symbols as in the $D = 4$ case in order to not clutter notation.

The Dyson–Schwinger equation is once more equation (4.1), only now with $D = 6 - 2\varepsilon$. This time, we define $\alpha := \lambda(4\pi)^{-3}$ to account for the additional factor 4π produced by the integration. Moreover, the 1-loop-integral is now proportional to q^2 but this factor is absorbed by projection onto the basis tensor such that again the tree level solution is $G^{(0)}(q^2) = 1$. Then, the coefficients of the renormalized Green function and the counterterm are given by the same recursion relations as above, namely equations (4.7), (4.8) and (4.11). The crucial difference is that for $f_n^{(k)}$ one now takes the value of the 6-dimensional primitive integral, as given in equation (B.3).

Once more, the anomalous dimension can be computed analytically from the Mellin transform of the 1-loop integral Appendix A. The Green function in kinematic

renormalization is [22]

$$G(\overline{x}) = \overline{x}^{\gamma(\alpha)}, \quad \gamma(\alpha) = \frac{\sqrt{5+4\sqrt{1+\alpha}}-3}{2}.$$

The functions $\overline{\gamma}_k(\alpha)$ are again computed from equation (4.9) using the appropriate $\overline{g}^{(m)}_{t,s}$. Like above, all $\overline{\gamma}_k(\alpha)$ are proportional to the corresponding $\gamma_k(\alpha)$ at least up to α^{25} and $k = 20$.

The series coefficients of $\overline{\gamma}_0(\alpha)$ can no longer be identified from tables right away but result (4.15), expressed in terms of $\gamma(\alpha)$, is a helpful starting point. Eventually, one arrives at

$$\begin{aligned}\overline{\gamma}_0(\alpha) &= 3\sqrt{3}\frac{e^{\frac{1}{2}(\sqrt{5+4\sqrt{1+\alpha}}-3)(1-2\gamma_E)}(\sqrt{5+4\sqrt{1+\alpha}}-3)\Gamma(\frac{5}{2}-\frac{1}{2}\sqrt{5+4\sqrt{1+\alpha}})}{\alpha((1+\alpha)(5+4\sqrt{1+\alpha}))^{\frac{1}{4}}\Gamma(-\frac{1}{2}+\frac{1}{2}\sqrt{5+4\sqrt{1+\alpha}})} \\ &= \frac{6\gamma}{\alpha}\sqrt{\frac{\mathrm{d}(6\gamma)}{\mathrm{d}\alpha}}e^{\gamma(1-2\gamma_E)}\frac{\Gamma(1-\gamma)}{\Gamma(1+\gamma)}. \end{aligned} \tag{5.1}$$

This has been verified symbolically to order α^{25}. Knowing $\overline{\gamma}_0(\alpha)$, the shifts between MS-bar- (resp. MS-) and MOM-renormalization are

$$\overline{\delta}(\alpha) = \overline{\gamma}_0^{\frac{1}{\gamma}} \quad \text{and} \quad \widehat{\delta}(\alpha) = (4\pi e^{-\gamma})^{-\frac{1}{2}}\overline{\delta}(\alpha).$$

The counterterm in MS for the 6-dimensional theory is

$$\begin{aligned}\widehat{Z}(\alpha,\varepsilon) = \exp\Bigg\{\frac{1}{\varepsilon}\Big(&2\sqrt{5+4\sqrt{1+\alpha}}-6-\frac{3}{2}\ln\alpha+\ln(108) \\ &+\frac{1}{2}\ln\frac{\sqrt{5+4\sqrt{1+\alpha}}-1}{\sqrt{5+4\sqrt{1+\alpha}}+1}+\frac{3}{2}\ln\frac{\sqrt{5+4\sqrt{1+\alpha}}-3}{\sqrt{5+4\sqrt{1+\alpha}}+3}\Big)\Bigg\}.\end{aligned}$$

This function fulfills equation (2.7). Furthermore, it has been checked to order α^{25} (resp. α^{10}) that $Z(\alpha,\varepsilon)$ reproduces $\overline{\gamma}_0$ via equation (3.8) for the pseudo-MOM and the true MOM scheme, respectively.

6. Kreimer's linear toy model

Both Dyson–Schwinger equations considered above were based on the same 1-loop primitive Feynman graph as an integral kernel. Our formalism is not restricted to that particular integral, for comparison we here examine the linear Dyson–Schwinger equation in a toy model of renormalization proposed by Dirk Kreimer [37]. It reads

$$\widehat{G}(\alpha,x) = 1 + (1-\widehat{\mathcal{R}})\alpha\int_0^\infty \frac{\mathrm{d}y(xy)^{-\varepsilon}}{1+y}\widehat{G}(\alpha,xy),$$

where again ε is a regularization parameter. There is no distinction between MS- and MS-bar schemes in the toy model. We retreat to a comparison between MS and pseudo-MOM.

The anomalous dimension, computed from the Mellin transform (2.19) and Appendix A, is

$$\gamma(\alpha) = -\frac{1}{\pi}\arcsin(\pi\alpha) = -\alpha - \frac{\pi^2}{6}\alpha^3 - \frac{3\pi^4}{40}\alpha^5 - \frac{5\pi^6}{112}\alpha^7 - \cdots.$$

It has been verified to order α^{30} that the symbolic calculation of $G(\alpha, x)$ in pseudo-MOM renormalization produces, in the limit $\varepsilon \to 0$, the expansion coefficients of $x^{\gamma(\alpha)}$ from equation (2.18).

For MS, using [36, A034255], the scaling factor is

$$\begin{aligned}\widehat{\gamma}_0(\alpha) &= 1 + \sum_{m=1}^{\infty} \alpha^m \sum_{t=1}^{m} \overline{g}_{t,0}^{(m)} = 1 + \left(\frac{\pi^2\alpha^2}{4}\right) + \frac{5}{2}\left(\frac{\pi^2\alpha^2}{4}\right)^2 + \cdots \\ &= (1-\pi^2\alpha^2)^{-\frac{1}{4}} = \sqrt{\frac{\mathrm{d}\gamma}{\mathrm{d}\alpha}}. \end{aligned} \tag{6.1}$$

From this, the change of the renormalization point can be computed using equation (3.6). One finds

$$\ln\widehat{\delta}(\alpha) = \frac{\pi\ln(1-\alpha^2\pi^2)}{4\arcsin(\alpha\pi)} = -\frac{\pi^2}{4}\alpha - \frac{\pi^4}{12}\alpha^3 - \frac{73\pi^6}{1440}\alpha^5 - \mathcal{O}(\alpha^7),$$

where the constant coefficient vanishes since for the toy model $f_0 = f_0^{(0)} = 0$.

The series coefficients of the toy model are somewhat easier than for the physical theory. This entails that in the expansion

$$Z(\alpha,\varepsilon) \equiv \exp\left(-\sum_{n=-1}^{\infty} z_n(\alpha)\cdot\varepsilon^n\right) \equiv \exp\left(\sum_{n=1}^{\infty} z'_n(\varepsilon)\cdot\alpha^n\right) \tag{6.2}$$

the first functions $z_n(\alpha)$ and $z'_n(\alpha)$ can be found symbolically. Some of them are quoted in Appendix C for the interested reader. They suggest that $Z(\alpha,\varepsilon) \in [0,1]$. As expected from equation (3.8), also the linear toy model fulfils

$$\begin{aligned} z_{-1} &= -[\varepsilon^{-1}]\ln Z = -\int_0^{\alpha}\frac{\mathrm{d}u}{u}\gamma(u), \\ z_0 &= -[\varepsilon^0]\ln Z = -\frac{1}{4}\ln(1-\alpha^2\pi^2) = \ln\overline{\gamma}_0(\alpha). \end{aligned}$$

The upshot from the three linear Dyson–Schwinger equations is that the series coefficients of the shift $\delta(\alpha)$ between MS and MOM are sufficiently tame that one can recognize the functional form. These functions are convergent power series for small couplings α.

7. The chain approximation in $D = 4$

As an example of a situation where MS and MOM cannot be related by a shift $\delta(\alpha)$, we consider the chain approximation. In it, the only allowed graphs consist of a chain of one-loop subgraphs inserted into one single primitive, but no further nestings. It is sometimes viewed as an intermediate step between the linear and the full recursive DSE, see for example [9]. We restrict here to the $D = 4$, $\varepsilon = 0$ case. The first function of the log-expansion in MOM is known to be

$$\gamma_1(\alpha) = -\sum_{n=1}^{\infty}(n-1)!\alpha^n = e^{-\frac{1}{\alpha}}\int_{-\frac{1}{\alpha}}^{\infty}\frac{\mathrm{d}t}{t}e^{-t},$$

where the resummed series is the incomplete Euler gamma function. Explicit computation of the higher $\gamma_t(\alpha)$ in MOM produces coefficients which can again be identified,

$$\gamma_{t\geq 1} = (-1)^t\frac{1}{t!}\sum_{n=t}^{\infty}(n-1)!\alpha^n, \quad k\gamma_k(\alpha) = -\alpha\cdot\alpha\partial_\alpha\gamma_{k-1}(\alpha)$$
$$\Rightarrow\ x\partial_x G(\alpha,x) = \gamma_1(\alpha) + (-\alpha)\alpha\partial_\alpha G(\alpha,x).$$

Although the last equation reminds us of Callan–Symanzik equation (2.13) for a beta function $\beta(\alpha) = -\alpha$, it is structurally different. The function $\gamma_1(\alpha)$ is not the anomalous dimension of this model in the conventional physical sense because it does not multiply $G(\alpha, x)$.

In minimal subtraction we find

$$\overline{\gamma}_0(\alpha) = 1 + 2a + \frac{11}{2}\alpha^2 + \Big(\frac{37}{3} + \frac{2}{3}\zeta(3)\Big)a^3 + \Big(\frac{169}{4} - \frac{1}{120}\pi^4 + \frac{1}{2}\zeta(3)\Big)a^4 + \cdots$$
$$=: \sum_{r=0}^{\infty} r_k\alpha^k.$$

The coefficients grow approximately $r_k \sim (k-1)!$. The higher expansion functions $\overline{\gamma}_{t>0}(\alpha)$ are purely rational. Empirically, the coefficients agree with [36, A010842], $c_n = (n-1)![x^{n-1}]\frac{e^{2x}}{x-1}$,

$$\overline{\gamma}_1(\alpha) = -\alpha - 3\alpha^2 - 10\alpha^3 - 38\alpha^4 - 168\alpha^5 - 872\alpha^6 - 5296\alpha^7 - 37200\alpha^8 - \cdots$$
$$= \sum_{n=1}^{\infty} c_n\alpha^n.$$

The higher $\overline{\gamma}_j$, but not $\overline{\gamma}_0$, satisfy the recursion $k\overline{\gamma}_k(\alpha) = -\alpha\cdot\alpha\partial_\alpha\overline{\gamma}_{k-1}(\alpha)$. As remarked below Lemma 3.1, it is possible for $\delta(\alpha)$ to exist even if both $\{\gamma_j\}$ and $\{\overline{\gamma}_j\}$ do not fulfil a Callan–Symanzik equation. But in the present case, explicit calculation using equation (3.2) shows that no $\delta(\alpha)$ exists. The fact that MOM and MS are not

related by any $\delta(\alpha)$ means that the chain-approximation is nonphysical in the sense that, for different renormalization schemes, it gives rise to measurably different Green functions.

8. Non-linear Dyson–Schwinger equation in $D = 4$

In the remainder of the paper we repeat the above analysis of the two physical models and the toy model for the case that the Dyson–Schwinger equation is non-linear. Namely, instead of $Q \equiv 1$ we insert the invariant charge (2.2),

$$Q(G(\alpha, x)) = (G(\alpha, x))^s, \tag{8.1}$$

where $s \in \{-5, \dots, +5\}$. It seems that the literature so far has mostly concentrated on the physically most relevant cases $s = 0$ (linear approximation, e.g., [22, 23, 29]) and $s = -2$ (one inverse Green function inserted into the kernel, e.g., [3–5, 9–12]). In our case, the corresponding power of G is inserted into *only one* edge of the primitive. The setup discussed in [3–5] is conceptually different from our $s = -3$ since it amounts to inserting one G^{-1} into each of the two internal edges. Compare our result (8.5) with [5, Table 1]. Also see [45, Chapter 5] for a discussion of how insertion into only a subset of the available edges is equivalent to including additional primitive kernels.

8.1. Computation of the coefficients

The MS-renormalized Dyson–Schwinger equation for the $D = 4$ model reads

$$\widehat{G}(\alpha, q^2/\mu^2) = 1 + \alpha(4\pi)^2(1 - \widehat{\mathcal{R}}) \int \frac{\mathrm{d}^D k}{(2\pi)^D} \frac{(\widehat{G}(\alpha, k^2/\mu^2))^{s+1}}{(k+q)^2 k^2}. \tag{8.2}$$

Note that as above we choose a sign $+\alpha$ in front of the integral. For $s = -2$, this is the model examined in [9, 11, 12], up to a factor -2 in the definition of α, see [12, (12)].

For a recursive computation of the coefficients, we once more introduce $\hat{x}$, $\overline{x}$ according to equation (4.5) and thereby switch from MS- to MS-bar-renormalization. The first order solution coincides with the one of the linear DSE, (4.4),

$$\overline{G}^{(1)}(\alpha, \overline{x}) = 1 + \alpha \sum_{t=0}^{1} \overline{x}^{-t\varepsilon} \sum_{w=-1}^{\infty} \overline{g}^{(1)}_{t,w} \varepsilon^w.$$

The index $^{(m)}$ in the linear case counts both the coradical degree (= number of recursive iterations of the solution) and the order in α (= loop number of the involved graphs). In the non-linear DSE, we truncate the series expansion of $(\widehat{G}(\alpha, \overline{x}))^{s+1}$

at order α^{m-1} so that $\widehat{G}^{(m)}(\alpha, \bar{x})$ again involves graphs with at most m loops. This choice is arbitrary but convenient because it saves one index.

The recursion formula for the next order is more complicated than in the linear case of Section 4.1. This is because the non-linear DSE (8.2) involves a non-trivial power of the Green function inside the integral which needs to be expanded both in α and in $\bar{x}^{-\varepsilon}$. Assume we know the order-m-solution in the form

$$\bar{G}^{(m)}(\alpha, \bar{x}) = 1 + \sum_{n=1}^{m} \alpha^n \sum_{u=0}^{n} \bar{x}^{-u\varepsilon} \sum_{s=-n}^{\infty} \bar{g}_{u,w}^{(n)} \varepsilon^w =: 1 + \sum_{n=1}^{m} \alpha^n \bar{G}_n(\bar{x}, \varepsilon),$$

where we defined functions $\bar{G}_n(\bar{x}, \varepsilon)$. They are universal for all m. Next, we write a generic expansion of the invariant charge (8.1) according to

$$\begin{aligned} \bar{G}^{(m)}(\alpha, \bar{x}) \cdot Q(\bar{G}^{(m)}(\alpha, \bar{x})) &\equiv (\bar{G}^{(m)}(\alpha, \bar{x}))^{s+1} \\ &=: 1 + \sum_{n=1}^{m} \alpha^n \sum_{t=0}^{n} \bar{x}^{-t\varepsilon} \bar{h}_t^{(n)}(\varepsilon). \end{aligned} \tag{8.3}$$

The helper functions $\bar{h}_t^{(n)}(\varepsilon)$ are Laurent series in ε with the highest pole order ε^{-n}. They are given by Faa di Bruno's formula and the binomial theorem, $B_{n,k}$ are Bell polynomials, see [2] and [17, p. 134]:

$$\begin{aligned} &\frac{1}{(\bar{G}^{(m)}(\bar{x}))^{-s-1}} \\ &\quad = \frac{1}{(-s-2)!} \sum_{n=0}^{\infty} \alpha^n \frac{1}{n!} \sum_{k=1}^{n} (-s-2+k)! B_{n,k}(1!\bar{G}_1, 2!\bar{G}_2, \ldots), \ s < -1 \\ &(\bar{G}^{(m)}(\bar{x}))^{s+1} \\ &\quad = (s+1)! \sum_{n=0}^{\infty} \alpha^n \frac{1}{n!} \sum_{k=0}^{s+1} \frac{1}{(s+1-k)!} B_{n,k}(1!\bar{G}_1, 2!\bar{G}_2, \ldots), \quad s > -1. \end{aligned} \tag{8.4}$$

Knowing the functions $\bar{h}_t^{(n)}(\varepsilon)$, one integrates sum (8.3) term-wise like in the linear case of Section 4.1 and obtains the next-order coefficients

$$\bar{g}_{1,w}^{(1)} = f_w^{(0)}, \quad \bar{g}_{u,w}^{(n)} = \sum_{r=-1}^{n+w-1} \left([\varepsilon^{w-r}] \bar{h}_{u-1}^{(n-1)} \right) f_r^{(u-1)}.$$

Finally, one obtains the next order solution of the DSE,

$$\bar{G}^{(m+1)}(\alpha, \bar{x}) = \bar{G}^{(1)}(\alpha, \bar{x}) + (1 - \widehat{\mathcal{R}}) \sum_{n=2}^{m+1} \alpha^n \sum_{u=1}^{n} \bar{x}^{-u\varepsilon} \sum_{w=-n}^{\infty} \bar{g}_{u,w}^{(n)} \varepsilon^w.$$

The MS-counterterm is included via coefficients $g^{(n)}_{0,s}$ as in the linear case (4.8). For the non-linear DSE, there is no simple pseudo-MOM scheme. In practice, it is sufficient to include terms $\propto \varepsilon^m$ if one is interested in the finite part of the Green function $G^{(m)}(\alpha, \overline{x})$ since every iteration potentially multiplies the result with ε^{-1}.

Of course, the established methods [4, 11, 31] are tremendously more efficient in computing the anomalous dimension in MOM. A power-series solution of the ODE (8.6) to order α^{100} can be obtained within seconds while the brute-force algorithm merely reaches α^{10} symbolically after several hours. But the computation of $\gamma(\alpha)$ is only a side effect of our algorithm since we are actually interested in $\ln \delta(\alpha)$.

All computations, also the extraction of series coefficients in the computation of $h^{(n)}_t$ and $g^{(n)}_{u,w}$, have been done with the computer algebra system MATHEMATICA 12.3. In practice, the computation is entirely limited by CPU time due to an explosion of series coefficients: In order to reach ε^0 at order α^{10}, we have to include terms up to ε^{10} in the intermediate steps. Further we produce pole terms up to ε^{-10} and contributions up to $x^{-10\varepsilon}$, each $g^{(10)}_{t,s}$ requires series reversion and series multiplication. If we were to go to α^{20}, we would have to include ε^{20} from the start, dramatically slowing down every intermediate step.

The higher the order, the higher powers of π^2 and the more different zeta values appear. Algebraic operations with these expressions are increasingly slow. This second problem can be circumvented by working with floating point numbers, but it turns out that each iteration loses several decimal digits of precision. We computed the first orders symbolically and then continued numerically.

Thirdly, expansions (8.4) are, for large n, much harder for negative s than for small positive s due to the summation boundaries. Therefore, we reach higher order for the positive s.

8.2. Results

The coefficients were computed symbolically up to α^{10} for an invariant charge (8.1) where $s \in \{-5, \ldots, +5\}$. The results are extended up to at least α^{20} numerically with at least 30 valid decimal digits. It was verified in all cases that the first three orders of the leading log expansion fulfil equation (2.20) and that equation (3.11) holds (for some function $\overline{\gamma}(\alpha)$).

The anomalous dimensions up to order α^8 are reported in Table 6 in Appendix E. Let the anomalous dimension be $\gamma(\alpha) = \sum_{n=0}^{\infty} c_n \alpha^n$ then the empirical values of Table 6 suggest

$$c_0 = 0, \quad c_1 = -1, \quad c_2 = -(s+1),$$
$$c_3 = -(1+s)(2+3s), \quad c_4 = -(s+1)(2s+1)(7s+5).$$

Further, for $s = 1$ the sequence is [36, A177384]. The case $s = -3$ produces

$$\gamma(\alpha) = -\alpha + 2\alpha^2 - 14\alpha^3 + 160\alpha^4 - 2444\alpha^5 + 45792\alpha^6 - 1005480\alpha^7 + 25169760\alpha^8 \mp \cdots \tag{8.5}$$

Compare this to [5, Table 1], in which $G(\alpha, x)$ is inserted into both the internal edges of the primitive. Our result (8.5) reproduces the purely rational part of the latter, but not the terms proportional to $\zeta(j)$.

The anomalous dimension considered so far, $\gamma(\alpha) =: \gamma^{\text{pert}}(\alpha)$, is the perturbative solution to the differential equation (2.19),

$$-(1 + \gamma(\alpha)(s\alpha\partial_\alpha + 1))\gamma(\alpha) = \alpha. \tag{8.6}$$

This ODE has also non-perturbative solutions [9, 10] of the form

$$\gamma^{\text{non-pert}}(\alpha) = \alpha^\beta \exp\Big(-\frac{\lambda}{\alpha}\Big)(1 + b^{(1)}\alpha + b^{(2)}\alpha^2 + \cdots). \tag{8.7}$$

We determine the unknown coefficients as follows.[1] The ansatz

$$\gamma(\alpha) = \gamma^{\text{pert}}(\alpha) + \gamma^{\text{non-pert}}(\alpha)$$

is inserted into equation (8.6) and the above coefficients c_j are used for γ^{pert}. The equation is then linearized in $\gamma^{\text{non-pert}}$. The resulting series in α has to vanish, this leads to the expressions listed in (D.1), especially $\lambda(s) = 1/s$, $\beta(s) = -(3 + 2s)/s$. For $s = -2$ we reproduce [9, (25)] up to different sign conventions regarding α, mentioned below equation (8.2).

The coefficients c_n of the perturbative solution of the non-linear DSE (8.6), grow factorially, which has been studied repeatedly [3,8,9,12]. The asymptotic behaviour of c_n is dictated by the non-perturbative solution of equation (8.7), see [1] (alternatively, use the methods of [3]), namely for $n \to \infty$

$$c_n \sim S(s) \cdot \frac{1}{\lambda(s)^n} \cdot \Gamma(n - \beta(s)) \times \Big(1 + \frac{\lambda(s) \cdot b^{(1)}(s)}{(n - \beta(s) - 1)} + \frac{\lambda(s)^2 \cdot b^{(2)}(s)}{(n - \beta(s) - 1)(n - \beta(s) - 2)} + \cdots\Big). \tag{8.8}$$

We computed 500 series coefficients of $\gamma^{\text{pert}}(\alpha)$ and extracted their asymptotic behaviour using order-70 Richardson extrapolation. This produced at least 50 significant digits and confirmed the expressions $\lambda(s)$, $\beta(s)$, $b^{(1)}(s)$, $b^{(2)}(s)$ and $b^{(3)}(s)$ listed

[1] The author thanks Gerald Dunne for suggesting this method, which has also been used in [10, Section 5.1].

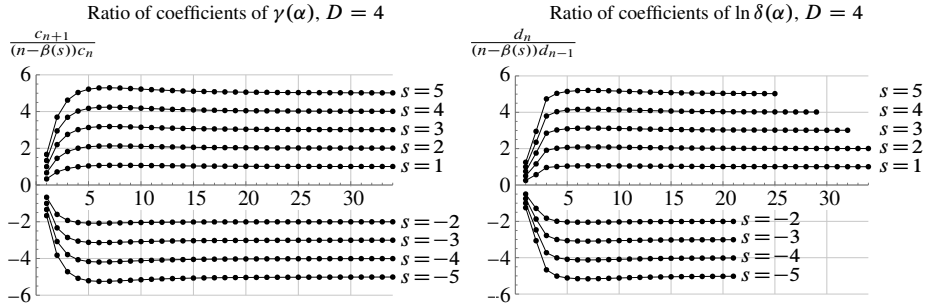

Figure 4. (a) Ratio of successive coefficients c_n of $\gamma(\alpha) = \sum c_n \alpha^n$ for the physical model in $D = 4$ dimensions. The denominator $(n - \beta(s))$ is chosen to match the known asymptotics (8.8). The ratio quickly converges towards the limit s, see equation (8.9). (b) Ratio of successive coefficients d_n of $\ln \delta(\alpha) = \sum_n d_n \alpha^n$. Seemingly, it converges to the same limit s as the ratio in (a). The computation is much harder for negative s, therefore only a lower order n is available.

in equation (D.1). The Stokes constant $S(s)$ is reported in Table 7 in Appendix E. One recognizes [9], $S(-2) = 1/(\sqrt{\pi} e)$ and also $S(-3) = 3/(\pi e^2)$, all other Stokes constants appear unfamiliar.[2]

To visualize the asymptotic behaviour, we consider the ratio

$$\frac{c_{n+1}/\Gamma(n+1-\beta(s))}{c_n/\Gamma(n-\beta(s))} \equiv \frac{c_{n+1}}{(n+\frac{3+2s}{s})c_n} = s - b^{(1)}(s)\frac{1}{n^2} + \mathcal{O}\Big(\frac{1}{n^3}\Big) \tag{8.9}$$

for $s \neq 0, -1$. There is no $1/n$ correction to this quantity, hence it converges quickly, as shown in Figure 4 (a).

The shift from MOM- to MS-bar-renormalization is computed as discussed in Section 3.1. The first coefficients are reported in Table 8, for example, for $s = -2$ one obtains

$$\begin{aligned}\overline{\gamma}_0(\alpha) &= 1 + 2\alpha - \frac{11}{2}\alpha^2 + \frac{88}{3}\alpha^3 - \Big(\frac{1781}{8} + \frac{\zeta(3)}{3}\Big)\alpha^4 \\ &\quad + \Big(\frac{42613}{20} + \frac{\pi^2}{150} - \frac{12\zeta(3)}{5}\Big)\alpha^5 - \mathcal{O}(\alpha^6), \\ \ln \overline{\delta}(\alpha) &= -2 + \frac{3}{2}\alpha - \frac{29}{6}\alpha^2 + \frac{94-\zeta(3)}{3}\alpha^3 - \Big(\frac{5573}{20} + \frac{\pi^4}{150} - \frac{7\zeta(3)}{5}\Big)\alpha^4 \mp \cdots .\end{aligned}$$

[2]The Stokes constant $S(s)$ was also computed for non-integer s. It appears to be a fairly smooth function of s, with zeros, as expected, at the points $s = -1$ and $s = 0$. Remarkably, inside the interval $(-1, 0)$ the function is oscillating and has additional zeros, accumulating near $s = 0$. This could be worth further study.

s	$n_{\max}$	$\widetilde{S}(s)/s$	$\widetilde{F}(s)$	$\widetilde{\beta}(s)$	$\widetilde{b}^{(1)}(s)$
5	24	-0.02532 ± 0.00037	4.987 ± 0.062	-3.59 ± 0.12	-2.61 ± 0.18
4	27	-0.02709 ± 0.00019	3.993 ± 0.036	-3.74 ± 0.08	-2.79 ± 0.11
3	32	-0.02749 ± 0.00011	2.997 ± 0.017	-3.99 ± 0.04	-3.10 ± 0.06
2	38	-0.02272 ± 0.00010	1.999 ± 0.009	-4.50 ± 0.03	-3.74 ± 0.05
1	38	-0.00541 ± 0.00009	0.999 ± 0.007	-6.00 ± 0.04	-5.97 ± 0.12
-2	21	0.2080 ± 0.0018	-1.998 ± 0.012	-1.49 ± 0.05	-0.74 ± 0.08
-3	21	0.1295 ± 0.0014	-2.995 ± 0.026	-1.99 ± 0.07	-1.10 ± 0.11
-4	21	0.0882 ± 0.0011	-3.993 ± 0.040	-2.24 ± 0.09	-1.30 ± 0.14
-5	21	0.0655 ± 0.0009	-4.991 ± 0.054	-2.40 ± 0.10	-1.43 ± 0.15

Table 1. Numerical findings of the growth parameters of $\ln \overline{\delta}(\alpha)$ in the $D = 4$ model of Section 8, according to equation (8.10). They are consistent with Table 7 and equation (D.1) in Appendix D. $\ln \overline{\delta}(\alpha)$ was computed including order $\alpha^{n_{\max}}$.

We write $\ln \overline{\delta}(\alpha) = \sum d_n \alpha^n$, where the coefficients d_n were computed up to order α^{10} symbolically and to at least order α^{20} numerically. As expected from equation (3.9), the constant coefficient is $d_0 = -2$ for all s. Similarly to equation (8.9), we examine the ratio of successive d_n, the result is shown in Figure 4 (b). We extract numerical estimates for the growth parameters in the ansatz

$$d_n \sim \widetilde{S}(s) \cdot \widetilde{F}(s)^n \cdot \Gamma(n - \widetilde{\beta}(s)) \Big(1 + \frac{\widetilde{b}^{(1)}(s)}{(n - \widetilde{\beta}(s) - 1)} + \cdots\Big) \tag{8.10}$$

by the following method: We use Richardson extrapolation [1, 39] of orders 2, 3, 4 and 5 and take their mean as the estimation and the largest absolute difference between any of these as uncertainty. Experiments with the coefficients c_n of $\gamma(\alpha)$ show that this procedure likely overestimates the uncertainties.

The results are reported in Table 1. They are consistent with

$$\widetilde{S}(s) = s \cdot S(s), \quad \widetilde{F}(s) = s \quad \text{and} \quad \widetilde{\beta}(s) = \beta(s) - 1$$

within around 1% relative uncertainty. Unlike the above analysis of γ, at this level of uncertainty our findings of "rational numbers" are to be understood as educated guesswork rather than numerical proofs. The estimates obtained for $\widetilde{b}^{(1)}(s)$ are too imprecise to deduce a formula at this point.

It turns out to be very useful to compare the coefficients of $\ln \delta(\alpha)$ to those of $\gamma(\alpha)$. To this end we compute the ratio $d_n/(s\lambda c_{n+1})$, where $s \cdot \lambda(s) = 1$ in our case. Using equation (8.10) with Table 1, we expect that $d_n/c_{n+1} \to 1$. As before, we use Richard-

s	$r_1(s)$	$r_2(s)$	$r_3(s)$	$r_4(s)$	$r_5(s)$
5	1.20002 ± 0.00012	0.0003 ± 0.0019	0.005 ± 0.031	0.09 ± 0.50	1.3 ± 7.9
4	1.25000 ± 0.00001	0.0000 ± 0.0002	0.000 ± 0.003	0.01 ± 0.05	0.18 ± 0.95
3	1.33333 ± 0.00001	0.0000 ± 0.0001	0.000 ± 0.001	0.01 ± 0.01	0.00 ± 0.02
2	1.50000 ± 0.00001	0.0000 ± 0.0001	0.000 ± 0.001	0.00 ± 0.01	0.00 ± 0.01
1	2.00000 ± 0.00001	0.0000 ± 0.0001	0.000 ± 0.001	0.00 ± 0.01	0.00 ± 0.01
−2	0.50000 ± 0.00001	0.0000 ± 0.0001	0.000 ± 0.001	0.00 ± 0.01	0.00 ± 0.02
−3	0.66667 ± 0.00001	0.0000 ± 0.0002	0.000 ± 0.002	0.01 ± 0.03	0.07 ± 0.39
−4	0.75001 ± 0.00004	0.0001 ± 0.0005	0.001 ± 0.007	0.02 ± 0.09	0.20 ± 1.24
−5	0.80001 ± 0.00006	0.0002 ± 0.0009	0.002 ± 0.012	0.03 ± 0.17	0.4 ± 2.3

Table 2. Parameters of the ratio d_n/c_{n+1} for $D = 4$ from equation (8.11); $r_{\geq 2}$ is consistent with zero.

son extrapolation of order 2, 3, 4 and 5 to determine the parameters in

$$\frac{d_n}{s\lambda c_{n+1}} \sim r(s) + r_1(s)\frac{1}{n} + r_2(s)\frac{1}{n^2} + \cdots, \quad n \to \infty. \tag{8.11}$$

We find $r(s) = 1$ with uncertainty smaller 10^{-5}. The numerical results for the corrections $r_j(s)$ are reported in Table 2. The relative uncertainties are much smaller than for the above parameters of equation (8.10). They suggest the simple formula

$$r(s) = 1 \quad \text{and} \quad r_1(s) = (s+1)/s.$$

Inserting this, surprisingly, the higher order corrections $r_{j\geq 2}(s)$ seem to vanish.

Together with the known behaviour of c_{n+1}, equation (8.8), $\lambda(s) = 1/s$ and $\beta(s) = -(3+2s)/s$, we conclude

$$\begin{aligned} d_n \sim\ & S(s) \cdot s \cdot \lambda(s)^{-n} \Gamma(n+1-\beta(s)) \\ & \times \left(1 + \frac{-\frac{1+3s+2s^2}{s^2}}{n-\beta(s)} + \frac{\frac{1+4s+4s^2-6s^3-7s^4}{2s^4}}{(n-\beta(s))(n-\beta(s)-1)} + \mathcal{O}\Big(\frac{1}{n^3}\Big)\right). \end{aligned} \tag{8.12}$$

The subleading coefficient is consistent with the value $\widetilde{b}^{(1)}(s)$ which we found in Table 1.

For the higher order corrections in Table 2, the uncertainties are increasing. If we nonetheless speculate that their vanishing is a general pattern, then we obtain

$$d_n = \left(1 + \frac{s+1}{sn}\right) \cdot c_{n+1} + e_n. \tag{8.13}$$

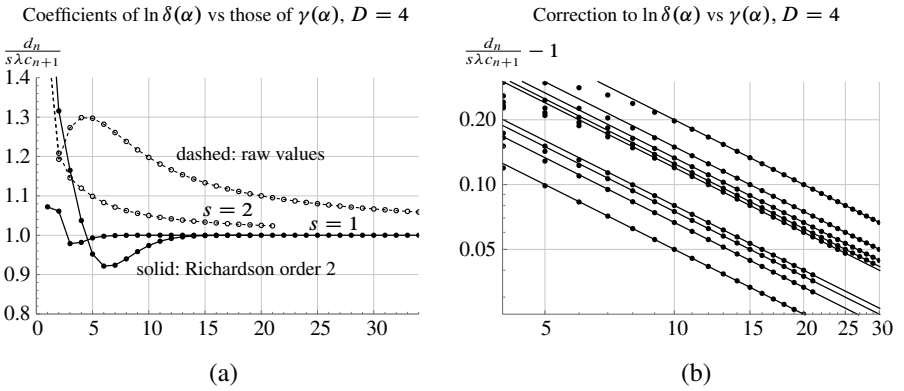

Figure 5. (a) Ratio of the coefficients of $\ln \delta(\alpha) = \sum d_n \alpha^n$ and $\gamma(\alpha) = \sum c_n \alpha^n$. Shown are two representative sequences, namely $s = -2$ and $s = 1$. For each of them, the dashed line indicates the raw values while the solid line is the order-2 Richardson extrapolation. The ratio d_n/c_{n+1} approaches the limit unity. (b) Correction to this ratio. The points are the values of $d_n/c_{n+1} - 1$ for the different s. Solid lines are the functions $(s+1)/sn$, they match the points surprisingly well even for low orders. The remaining difference falls of faster than $1/n^2$.

The numerical values suggest that the remainder e_n falls off faster than geometrically, see Figure 6 (a). Using the ring of factorially divergent power series [8], this asymptotic statement can be translated to a relation between the corresponding generating functions:[3]

$$\ln \overline{\delta}(\alpha) = \frac{\gamma(\alpha)}{\alpha} + \frac{s+1}{s} \int_0^\alpha \frac{\mathrm{d}a}{a} \Big(\frac{\gamma(a)}{a} - c_1 \Big) + f(\alpha), \quad s \neq 0. \tag{8.14}$$

Figure 6 (b) shows the coefficients of the function

$$f(\alpha) := \sum_{n=1}^{\infty} f_n \alpha^n,$$

they seemingly grow geometrically, not factorially. This indicates that $f(\alpha)$ is a convergent power series around $\alpha = 0$. The growth rate is reported in Table 8 in Appendix E. The coefficients of the function $f(\alpha)$ contain zeta values, which appear in $\ln \overline{\delta}(\alpha)$ but not in $\gamma(\alpha)$. The author has not succeeded in finding a closed formula.

A conclusion of Section 8 is that the factorial growth, or, equivalently, the leading non-perturbative contribution, of the shift function $\delta(\alpha)$ is surprisingly similar to the behaviour of the anomalous dimension $\gamma(\alpha)$.

[3] The author thanks Michael Borinsky for pointing out this implication of equation (8.13).

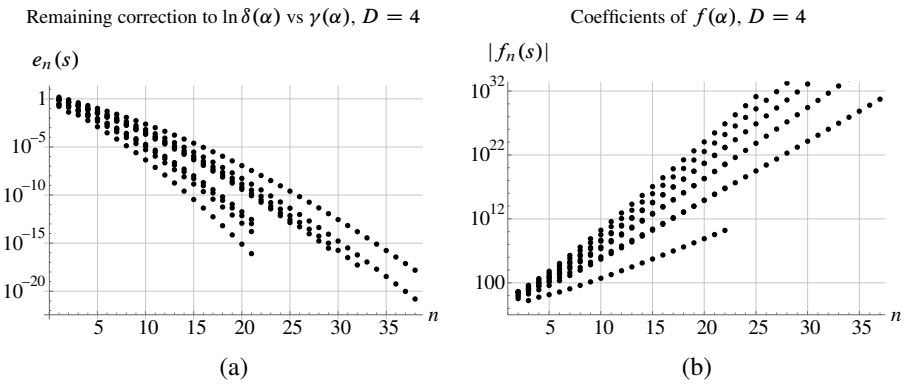

Figure 6. (a) Remainder coefficients e_n from equation (8.13), for the different values of s. This is a logarithmic plot, they decay faster than exponentially. (b) Coefficients of the function $f(\alpha)$ in equation (8.14). The data points overlap for different s. The coefficients grow exponentially, which suggests that $f(\alpha)$ is an analytic function.

9. Non-linear Dyson–Schwinger equation in $D = 6$

Following the procedure of Section 8.1, we also evaluate the 6-dimensional model of Section 5 for various powers $s \in \{-5, \dots, +5\}$ in the invariant charge (8.1).

The leading log functions H_1, H_2, H_3 are as expected from equation (2.20). The anomalous dimension $\gamma(\alpha)$ contains only rational coefficients for all values of s. Up to the computed symbolic precision α^{12}, they fulfil the ODE (2.19), which here takes the form

$$(3 + \gamma(s\alpha\partial_\alpha + 1))(2 + \gamma(s\alpha\partial_\alpha + 1))(1 + \gamma(s\alpha\partial_\alpha + 1))\gamma = \alpha. \tag{9.1}$$

The perturbative solution $\gamma^{\text{pert}}(\alpha) = \sum_{j=0}^{\infty} c_j \alpha^j$ can be computed to high order from this ODE, the first coefficients are

$$c_1 = \frac{1}{6}, \quad c_2 = -\frac{11(s+1)}{216},$$
$$c_3 = \frac{(s+1)(206+291s)}{7776},$$
$$c_4 = -\frac{(s+1)(4711+14887s+11326s^2)}{279936}.$$

We use these coefficients, insert the non-perturbative ansatz (8.7) into equation (9.1), linearize, and solve for the parameters β, λ, $b^{(1)}$, $b^{(2)}$, $b^{(3)}$. Equation (9.1) is of third order, unlike in the case $D = 4$, we find three linearly independent solutions (D.2). In ansatz (8.7), the solution with smallest absolute λ is dominant, this is the first entry of vectors (D.2).

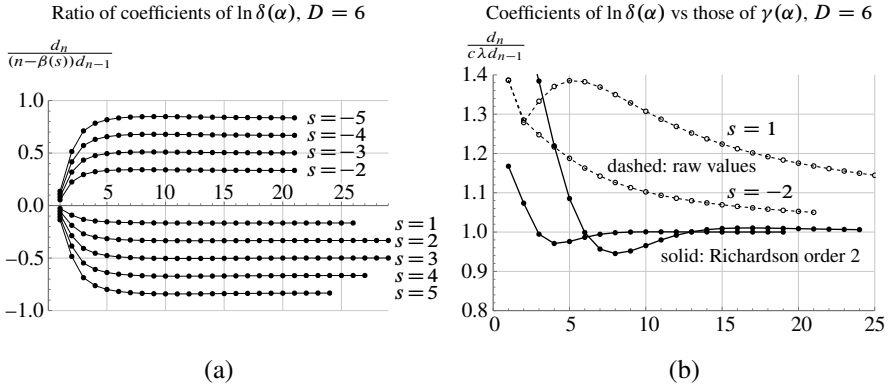

Figure 7. (a) Ratio of successive coefficients d_n of $\ln \delta(\alpha)$, divided by the assumed leading asymptotic behaviour from equation (D.2), for $D = 6$. This quantity quickly approaches the limit $-s/6$. (b) Ratio between the coefficients d_n of $\ln \delta(\alpha)$ and the coefficients c_{n+1} of $\gamma(\alpha)$. Compared to Figure 5 (a), the Richardson extrapolation converges slower, indicating a significant $1/n^2$-correction, see Table 4.

With these parameters, the series coefficients c_n of the perturbative solution grow according to equation (8.8). We have confirmed this behaviour numerically from the first 500 coefficients c_n for $s \in \{-5, \dots, +5\}$. The Stokes constant $S(s)$ is reported in Table 9, we reproduce the value [10, (15)] for $s = -2$. Like equation (8.9), the ratio of successive coefficients $c_{n+1}/((n - \beta_1(s))c_n)$ is constant up to quadratic corrections.

The power series coefficients of the shift $\ln \widehat{\delta}(\alpha)$ have been computed symbolically up to order α^{10}, the leading ones are reported in Table 10 in Appendix E. The numerical computation extends further, depending on s. The ratio of successive coefficients, with the same normalization as for $\gamma(\alpha)$, is shown in Figure 7 (a). The plot suggests that c_n grow at a similar rate as d_n.

As explained in Section 8.2, we extracted numerical estimates of the parameters in equation (8.10). They are given in Table 3 and are consistent with $\widetilde{S}(s) = s \cdot S(s)$, $\widetilde{F}(s) = -s/6$ and $\widetilde{\beta}(s) = \beta_1(s) - 1$. Once more, the relative uncertainty of about 1% of these values is too large to rigorously identify the rational values.

The ratio $d_n/(s\lambda c_{n+1}) = d_n/(-6c_{n+1})$ is depicted in Figure 7 (b) for two values of s. The asymptotic parameters, according to equation (8.11), are given in Table 4. Unlike for $D = 4$, this ratio does not converge particularly quickly. A fit suggests that $r_1(s) = (2.12 + 2.15s)/s$, but the uncertainties are too large to identify the numbers as rational. This is reflected by the large absolute values we obtain for the $1/n^2$-correction $r_2(s)$, see Table 4. In $D = 4$, this correction vanished and therefore allowed us to extract $r_1(s)$ precisely.

s	$n_{\max}$	$10^6 \cdot \widetilde{S}(s)/s$	$\widetilde{F}(s)$	$\widetilde{\beta}(s)$
5	24	-50.1 ± 4.5	-0.833 ± 0.018	-7.00 ± 0.37
4	27	-34.5 ± 2.4	-0.666 ± 0.012	-7.25 ± 0.23
3	29	-16.6 ± 1.2	-0.500 ± 0.007	-7.72 ± 0.19
2	29	-2.97 ± 0.28	-0.333 ± 0.006	-8.68 ± 0.26
1	26	-0.0054 ± 0.0015	-0.167 ± 0.006	-11.64 ± 0.75
-2	21	87900 ± 1600	0.333 ± 0.005	-2.92 ± 0.12
-3	21	18000 ± 560	0.500 ± 0.009	-3.90 ± 0.21
-4	21	6690 ± 290	0.666 ± 0.013	-4.39 ± 0.26
-5	21	3410 ± 180	0.833 ± 0.018	-4.69 ± 0.29

Table 3. Numerical findings of the growth parameters of $\ln \overline{\delta}(\alpha)$ in the $D = 6$ model of Section 9, according to equation (8.10). They are consistent with equation (D.2) and Table 9 in Appendix E.

s	$r(s)$	$r_1(s)$	$r_2(s)$
5	1.0010 ± 0.0017	2.573 ± 0.072	-6.91 ± 0.84
4	1.0007 ± 0.0019	2.685 ± 0.072	-7.3 ± 1.4
3	1.0007 ± 0.0024	2.863 ± 0.078	-8.4 ± 1.8
2	1.0010 ± 0.0026	3.21 ± 0.11	-11.2 ± 1.8
1	1.0032 ± 0.0048	4.22 ± 0.23	-22.3 ± 1.3
-2	1.0000 ± 0.0002	1.083 ± 0.003	-1.10 ± 0.34
-3	1.0002 ± 0.0004	1.441 ± 0.012	-1.80 ± 0.07
-4	1.0003 ± 0.0007	1.619 ± 0.018	-2.33 ± 0.16
-5	1.0004 ± 0.0008	1.726 ± 0.022	-2.71 ± 0.22

Table 4. Parameters of the ratio $d_n/(-6c_{n+1})$ for $D = 6$ from equation (8.11).

All in all, we cannot clearly identify the subleading corrections of d_n in the $D = 6$ model, but the findings at least suggest that the leading growth coincides with the one of c_{n+1}, using $\lambda(s) = -6/s$ and $\beta(s) = -(35 + 29s)/(6s)$ from equations (D.2), i.e.,

$$d_n \sim S(s) \cdot s \cdot \left(-\frac{s}{6}\right)^n \Gamma\left(n + 1 + \frac{35 + 29s}{6s}\right). \tag{9.2}$$

10. Non-linear toy model

We solved the non-linear toy model DSE for $s \in \{-5, \ldots, +4\}$ symbolically to order α^{16}. The leading log functions H_1, H_2 and H_3 agree with the general formula (2.20) of [32] for the appropriate choice $c_1 = 1, c_2 = 0, c_3 = \pi^2/2$ and for all values of s. Especially, for $s = -2$, we confirm H_1 from [37, Corollary 3.6.4] and $H_2 = H_4 = H_6 = 0$.

s	$n_{\max}$	$\widetilde{S}(s)/s$	$\widetilde{F}(s)$	$\widetilde{\beta}(s)$
4	23	-0.389 ± 0.010	3.985 ± 0.081	-2.50 ± 0.21
3	23	-0.485 ± 0.015	2.988 ± 0.068	-2.68 ± 0.24
2	23	-0.612 ± 0.023	1.991 ± 0.059	-3.02 ± 0.31
1	23	-0.572 ± 0.037	0.996 ± 0.056	-4.09 ± 0.56
-2	23	0.6382 ± 0.0067	1.997 ± 0.012	-0.991 ± 0.050
-3	23	0.5275 ± 0.0076	2.994 ± 0.024	-1.322 ± 0.071
-4	23	0.4202 ± 0.0069	3.991 ± 0.037	-1.488 ± 0.082
-5	23	0.3443 ± 0.0060	4.988 ± 0.051	-1.588 ± 0.088

Table 5. Numerical findings of the growth parameters of $\ln \overline{\delta}(\alpha)$ in the toy model, according to equation (8.10). $\widetilde{S}(s)$ is consistent with Table 11.

The symbolic results for the anomalous dimension fulfil equation (2.19),

$$-\frac{\sin(u)}{u}\Big|_{u\to-\gamma(1+s\alpha\partial_\alpha)}\gamma(\alpha)=\alpha. \tag{10.1}$$

Unlike the ODEs (8.6) and (9.1), equation (10.1) contains a pseudo-differential operator.

We computed a symbolic perturbative power series solution $\gamma(\alpha)=\sum c_n\alpha^n$ of equation (10.1) to order 450 and extracted the asymptotic behaviour. The result has the form (8.8) for n odd. We find $\beta(s)=-(2+s)/s$, numerical values of the constants $S(s)$, $b^{(1)}(s)$ and $b^{(2)}(s)$ are given in Table 11 in Appendix E. We did not recognize these numbers apart from the Stokes constant $S(-2)=2/\pi$.

By (3.9), the shift $\ln\delta(\alpha)=\sum d_n\alpha^n$ does not have a constant term in the toy model. The first coefficients for the shift are reported in Table 12 in Appendix E, while Table 5 contains the numerical estimates for their growth parameters.

The toy model has the property that both c_n and d_n vanish for even n. This is problematic for two reasons: Firstly, although we computed numerically the order α^{23}, we only get 12 non-vanishing coefficients of $\ln\delta(\alpha)$. Secondly, we cannot compute the ratio d_n/c_{n+1} and therefore not use the trick which allowed us to extract the behaviour of d_n in the $D=4$ physical model, see Section 8.

To visualize the coefficients d_n of $\ln\delta(\alpha)$, we consider the following two ratios for odd n:

$$\begin{aligned} R^{(\delta)} &:= \sqrt{\frac{d_{n+2}}{(n-\beta(s)+1)(n-\beta(s)+2)d_n}}, \\ R^{(\delta/\gamma)} &:= \frac{d_n}{s\cdot(n-\beta(s)+1)c_n}. \end{aligned} \tag{10.2}$$

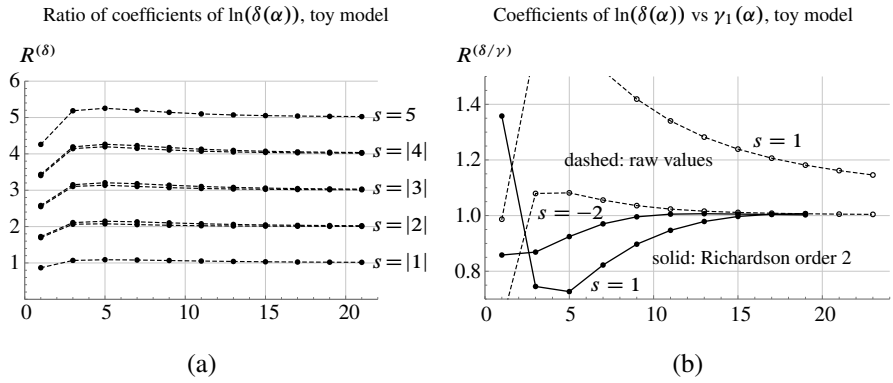

Figure 8. (a) Ratio (10.2) of successive coefficients of $\ln \delta(\alpha)$. The ratio visibly approaches $|s|$, Richardson extrapolation (not shown) confirms this. (b) Ratio $R^{(\delta/\gamma)}$ between coefficients of $\ln \delta(\alpha)$ and $\gamma(\alpha)$ and its order-2-Richardson extrapolation. The limit seems to be unity, but knowing only 12 terms the uncertainty is large. Compare the first 12 terms of Figure 5 (a).

Figure 8 (a) shows that $R^{(\delta)}$ approaches the limit $|s|$, which suggests that d_n scale asymptotically $\sim s^n \Gamma(n - \beta(s) + 1)$, with (approximately) the same $\beta(s)$ as the coefficients c_n of $\gamma(\alpha)$. The quantity $R^{(\delta/\gamma)}$ allows us to fix the Stokes constant, it is shown in Figure 8 (b). The limit of $R^{(\delta/\gamma)}$ is 1.00 ± 0.02, suggesting that the Stokes constant agrees with the one of $\gamma(\alpha)$. In Table 5, the direct estimates of the asymptotic growth are reported. All in all, it seems that the coefficients of $\ln \delta(\alpha)$ grow factorially according to

$$d_n \sim S(s) s^{n+1} \Gamma(n + (2 + 2s)/s). \tag{10.3}$$

We did not try to determine subleading corrections.

10.1. Exact solutions

We end this paper with a curious empirical observation. First, for $s = -\frac{1}{2}$, the perturbative anomalous dimension in MOM for $\varepsilon \to 0$ turns out to be $\gamma(\alpha) = -\alpha$, which was checked up to $\mathcal{O}(\alpha^{500})$. Moreover, in MS for $s = -2$, we find $\overline{\gamma}(\alpha) = -\alpha$ at least up to order α^{18}. By construction, the latter is true even for $\varepsilon \neq 0$. If we assume that there are indeed no higher order terms in α, then a particularly simple Callan–Symanzik equation (2.13) follows.

Firstly, consider the case $s = -1$ in MOM which clearly has $\gamma(\alpha) = -\alpha$ since the DSE is not even recursive. The beta function is $\beta(\alpha) = s\gamma(\alpha) = +\alpha$ and the

Callan–Symanzik equation becomes

$$\partial_{\ln x} G(\alpha, x) = -\alpha G(\alpha, x) + \alpha^2 \partial_\alpha G(\alpha, x).$$

The general solution of this partial differential equation is

$$G(\alpha, x) = \alpha F_{-1}\Big(\ln(x) - \frac{1}{\alpha}\Big),$$

where F_{-1} is an arbitrary function. The requirement $\gamma(\alpha) = -\alpha$ together with the boundary condition $G(\alpha, 1) = 1$ fixes $F_{-1}(u) = -u$.

The Callan–Symanzik equation for $s = -\frac{1}{2}$ has the general solution

$$G(\alpha, x) = \alpha^2 F_{-\frac{1}{2}}\Big(\ln(x) - \frac{2}{\alpha}\Big).$$

The condition $\gamma(\alpha) = -\alpha$ translates to $\partial_u F_{-\frac{1}{2}}(u) = \frac{1}{2}u$ and we find

$$G(\alpha, x) = \frac{1}{4}\alpha^2 \ln(x)^2 - \alpha \ln(x) + 1.$$

Both MOM-results are consistent with equation (2.16).

The case $s = -2$ in MS leads to a similar general solution,

$$\bar{G}(\alpha, x) = \sqrt{\alpha}\, \bar{F}_{-2}\Big(\ln(x) - \frac{1}{2\alpha}\Big).$$

This time we cannot fix the function $\bar{F}_{-2}$ because the anomalous dimension $\bar{\gamma}(\alpha)$ is not simply the derivative of $\bar{G}(\alpha, x)$, see equation (3.4). The shift $\delta(\alpha)$ between MS and MOM is given by the inverse function,

$$\ln \delta(\alpha) = -(\bar{F}_{-2})^{-1}\Big(\frac{1}{\sqrt{\alpha}}\Big) - \frac{1}{2\alpha}.$$

These two non-linear DSEs illustrate that it can be worth trying to solve a DSE both in MOM and in MS, but also that going from one scheme to another requires a truly new, independent calculation and is not trivial even if one happens to know an exact solution in one of the schemes.

11. Conclusion

We have discussed how a Green function in minimal subtraction (MS) is related to its corresponding Green function in kinematic renormalization (MOM). To this end, we have examined and used various relations between the renormalization group functions and Z-factors to find the shift of the renormalization point, see Section 3.

We have computed the series coefficients of $\delta(\alpha)$ symbolically and numerically for propagator-type Dyson–Schwinger equations with three different kernels. In some cases, we identified the coefficients' algebraic formulas. Whenever there is an overlap with earlier literature, our results agree with the ones reported. The key outcomes of the present work are:

(1) We have shown for single, propagator-type Dyson–Schwinger equations, that their solutions in MS, MS-bar and MOM schemes agree to all orders in perturbation theory if one chooses a suitable kinematic renormalization point $\delta(\alpha)$, which is a power series in α, see Theorem 3.4.

(2) In the linear examples, the factors $\delta(\alpha)$ between the renormalization points have been deduced in closed form as $\delta(\alpha) = \gamma_0^{1/\gamma}$, see (4.15), (5.1) and (6.1). The result is finite in perturbation theory and proportional to $\sqrt{\partial_\alpha \gamma(\alpha)}$. It also encodes information about the MOM-solution for $\varepsilon \neq 0$, see equation (3.7).

(3) For non-linear DSEs, series coefficients for $\gamma(\alpha)$ and $\ln \delta(\alpha)$ have been computed for several different exponents s in the invariant charge $Q = G^s$. The results are highly regular in s. The first symbolic coefficients of $\ln \delta(\alpha)$ are collected in Appendix E.

(4) The coefficients d_n of $\ln \delta(\alpha)$ seem to grow factorially. In all cases, we find $d_n \sim S \cdot s \cdot \lambda^{-n} \cdot \Gamma(n + 1 - \beta)$, where $S(s)$, $\lambda(s)$ and $\beta(s)$ are the growth parameters of the corresponding anomalous dimension $\gamma(\alpha)$, equations (8.12), (9.2) and (10.3). This suggests that $\delta(\alpha)$ receives non-perturbative contributions of the same type as does the anomalous dimension $\gamma(\alpha)$ [9, 10]. The resemblance is particularly striking in the $D = 4$ model, equation (8.14).

(5) The chain approximation Section 7 is an example of a Green function which does not originate from a DSE and cannot be transformed between MS and MOM. This calls into question the physical validity of this approximation since different renormalization schemes will produce truly different renormalized Green functions.

(6) Our numerical data suggests some new tentative exact results: The Stokes constant for $s = -3$ in the $D = 4$ model seems to be $S(-3) = 3/(\pi e^2)$, see Section 8.2. And for the non-linear toy model at $s = -2$ in MS and for $s = -\frac{1}{2}$ in MOM, the anomalous dimension appears to be $\gamma(\alpha) = -\alpha$. This allows one to solve the Callan–Symanzik equation up to one unknown function, which in the MOM-case can be determined uniquely, see Section 10.1.

All examples indicate that there is a significant shift factor $\delta(\alpha)$ between the mass scale μ of MS-renormalization and the corresponding kinematic renormalization point. By equation (3.9), the shift does not vanish in the limit of vanishing coupling. Consequently, one should be careful not to confuse the mass scale μ of

MS-renormalization with a kinematic renormalization point, even in the most well-behaved cases and even for "small coupling".

For the linear DSEs, we have found an explicit map $\gamma(\alpha) \mapsto \ln \delta(\alpha)$ in equations (4.15), (5.1) and (6.1). For the non-linear DSEs, this connection is not quite so simple. Intuitively, the identical asymptotic growth hints at the possibility to find an explicit map as well. Indeed, for the $D = 4$ case, assuming that our empirical findings hold to all orders, equation (8.14) reproduces the factorial growth of d_n and therefore the non-perturbative behaviour. The analytic remainder function $f(\alpha)$ in this case remains to be identified.

A. Mellin transforms

The Mellin transform is by definition the value of the primitive integral where one of the propagators is raised to a power $1 + \rho$, evaluated at unity external momentum. Factors of 4π from the Fourier transform are implicitly absorbed into the mass scale in the main text, therefore they are left out from the Mellin transform. For the 4-dimensional respectively 6-dimensional propagator,

$$M(\rho) = \int \frac{\mathrm{d}^4 k \, (k^2)^{-\rho}}{(k+q)^2 k^2}\Big|_{q^2=1} = \frac{1}{\rho(1-\rho)},$$
$$M(\rho) = \int \frac{\mathrm{d}^6 k \, (k^2)^{-\rho}}{(k+q)^2 k^2}\Big|_{q^2=1} = -\frac{1}{\rho(1-\rho)(2-\rho)(3-\rho)}.$$

The Mellin transform in the toy model is

$$M(\rho) = \int_0^\infty \frac{\mathrm{d}y \, y^{-\rho}}{x+y}\Big|_{x=1} = \frac{\pi}{\sin(\pi\rho)}.$$

B. Series expansion of the primitive graphs

We are interested in the series expansion in ε of the integral

$$\begin{aligned} I_D^{(k)}(q) &:= \int \frac{\mathrm{d}^D p}{(2\pi)^D} \frac{1}{(p+q)^2 (p^2)^{1+k\varepsilon}} \\ &= (4\pi)^{-\frac{D}{2}} (q^2)^{\frac{D}{2}-2-k\varepsilon} \frac{\Gamma(-\frac{D}{2}+2+k\varepsilon)\Gamma(\frac{D}{2}-1)\Gamma(\frac{D}{2}-1-k\varepsilon)}{\Gamma(1+k\varepsilon)\Gamma(D-2-k\varepsilon)} \\ &=: (4\pi)^{-\frac{D}{2}} (q^2)^{\frac{D}{2}-2-k\varepsilon} e^{-\gamma_E \varepsilon} \sum_n f_n^{(k)} \varepsilon^n. \end{aligned}$$

The factors of q^2 must not be expanded into logarithms, in order to be integrated in the next iteration. Furthermore, we do not expand the (4π) and factor out $e^{-\gamma_E \varepsilon}$

because both can conveniently be absorbed into the momentum. It remains to expand the gamma functions using

$$\Gamma(x+1) = x\Gamma(x), \quad \Gamma(1+\varepsilon) = \exp\left(-\gamma_E \varepsilon + \sum_{m=2}^{\infty} \frac{(-\varepsilon)^m}{m} \zeta(m)\right).$$

In $D = 4 - 2\varepsilon$ dimensions one obtains

$$\begin{aligned}\Gamma :=& \frac{\Gamma((k+1)\varepsilon)\Gamma(1-(k+1)\varepsilon)\Gamma(1-\varepsilon)}{\Gamma(1+k\varepsilon)\Gamma(2-(k+2)\varepsilon)} \\ =& \frac{1}{(k+1)(1-(k+2)\varepsilon)\varepsilon} \exp\left(-\gamma_E \varepsilon + \sum_{m=2}^{\infty} T_m^{(k)} \varepsilon^m\right), \end{aligned} \tag{B.1}$$

where

$$T_m^{(k)} := (m-1)!((-1)^m(k+1)^m + (k+1)^m + 1 - (-k)^m - (k+2)^m)\zeta(m).$$

Expanding the prefactor in a geometric series and leaving out $e^{-\gamma_E \varepsilon}$,

$$f_n^{(k)} = \sum_{t=-1}^{n} \frac{(k+2)^{t+1}}{k+1} \frac{1}{(n-t)!} \sum_{m=0}^{n-t} B_{n-t,m}(0, T_2^{(k)}, T_3^{(k)}, \ldots, T_{n-t+1-m}^{(k)}). \tag{B.2}$$

Here $B_{n,k}$ are incomplete Bell polynomials, [2] and [17, p. 134]. For $D = 6 - 2\varepsilon$ dimensions, observe

$$\frac{\Gamma(-1+(k+1)\varepsilon)\Gamma(2-\varepsilon)\Gamma(2-(k+1)\varepsilon)}{\Gamma(1+k\varepsilon)\Gamma(4-(k+2)\varepsilon)} = \frac{\varepsilon - 1}{(3-(k+2)\varepsilon)(2-(k+2)\varepsilon)} \cdot \Gamma.$$

The gamma functions on the right-hand side are the same as in $D = 4 - 2\varepsilon$, consequently their series expansion is again given by the polynomials $T_m^{(k)}$ from equation (B.1),

$$\begin{aligned} f_n^{(k)} =& \sum_{t=-1}^{n} \left(-(k+1) + \frac{k}{2^{t+1}} - \frac{k-1}{3^{t+2}}\right) \frac{(k+2)^t}{2(k+1)} \frac{1}{(n-t)!} \\ & \times \sum_{m=0}^{n-t} B_{n-t,m}(0, T_2^{(k)}, \ldots, T_{n-t+1-m}^{(k)}). \end{aligned} \tag{B.3}$$

In the toy model, the relevant integral and its series expansion are

$$\begin{aligned} \int_0^\infty \frac{\mathrm{d}y\, y^{-(k+1)\varepsilon}}{1+y} =& \frac{\pi}{\sin(\pi(k+1)\varepsilon)} = \Gamma((k+1)\varepsilon)\Gamma(1-(k+1)\varepsilon) \\ =:& \sum_{n=-1}^{\infty} f_n^{(k)} \varepsilon^n. \end{aligned}$$

The Bernoulli numbers B_n vanish when $n > 1$ is odd, therefore we can write

$$f_n^{(k)} := \frac{1}{(k+1)} \sum_{m=0}^{n+1} \frac{1}{(n+1)!} B_{n+1,m}(0, T_2^{(k)}, \dots, T_{n+2-m}^{(k)}),$$
$$T_n^{(k)} := (2\pi(k+1))^n \frac{|B_n|}{n}.$$

C. Kinematic counterterm of the linear toy model

These are the first coefficients of equation (6.2) for the toy model. Define $A := \alpha^2\pi^2$.

$$z_1 = \frac{\alpha\pi^2(4+A)}{24(1-A)^{\frac{3}{2}}}, \qquad z_2 = \frac{\alpha^2\pi^4(3+2A)}{16(1-A)^3},$$
$$z_3 = \frac{\alpha\pi^4(112+2240A+2919A^2+254A^3)}{5760(1-A)^{\frac{9}{2}}},$$
$$z_4 = \frac{\alpha^2\pi^6(36+515A+900A^2+240A^3+4A^4)}{384(1-A)^6},$$
$$z_5 = \frac{\alpha\pi^6}{967680(1-A)^{\frac{15}{2}}} \cdot (1984+522152A+6074220A^2+12882535A^3 + 6095260A^4+511956A^5+1768A^6),$$
$$z_6 = \frac{\alpha^2\pi^8}{11520(1-A)^9} \cdot (471+42058A+428661A^2+1041030A^3 + 715270A^4+129414A^5+4092A^6+4A^7).$$

All explicitly determined functions $z_n(\alpha)$ for $n > 0$ behave qualitatively similar: They diverge like $(1-A)^{-\frac{3}{2}n}$ as $\alpha\pi \to 1$ and are positive for $0 \le \alpha < \frac{1}{\pi}$. In this interval, they give rise to a finite Z-factor. The other coefficients in equation (6.2) are

$$z_1' = \frac{1}{\varepsilon} + \frac{\pi^2}{6}\varepsilon + \frac{7\pi^4}{360}\varepsilon^3 + \dots = -\frac{1}{\varepsilon}\sum_{n=0}^{\infty} \frac{(-1)^n(4^n-2)B_{2n}}{(2n)!}\pi^{2n}\varepsilon^{2n}$$
$$= \pi\left(\cot\left(\frac{\pi}{2}\varepsilon\right) - \cot(\varepsilon\pi)\right), \quad z_2' = \frac{\pi^2}{4}\frac{1}{\cos^2(\frac{\pi}{2}\varepsilon)\cos(\varepsilon\pi)},$$
$$z_3' = \frac{\pi^3}{12}\frac{1-2\cos(2\pi\varepsilon)+2\cos(\pi\varepsilon)}{(2\cos(\pi\varepsilon)+3\cos(3\pi\varepsilon))\sin(\frac{\pi}{2}\varepsilon)\cos^3(\frac{\pi}{2}\varepsilon)},$$
$$z_4' = -\frac{\pi^4}{4}\frac{\cos(\pi\varepsilon)+2\sin^2(\pi\varepsilon)}{\cos^4(\pi\varepsilon)(\cos(\pi\varepsilon)-4\cos^2(\pi\varepsilon)\cos(2\pi\varepsilon)+\cos(3\pi\varepsilon))}.$$

The functions $z_n'(\varepsilon)$ are positive for small positive ε. They change sign at their poles but probably, there are other continuations of the series expansion around $\varepsilon = 0$

beyond the poles, which stay positive. For example,

$$z_2'(\varepsilon) = \frac{\pi^2}{2}\Big(\frac{1}{\sin^2(\pi\varepsilon)} - \frac{|\cot(\pi\varepsilon) - \cot(\frac{\pi}{2}\varepsilon)|^3}{|\cot(\pi\varepsilon)|}\Big)$$

is always positive and reduces to the above form of z_2' for $|\varepsilon| < 0.5$. If this holds for all z_n' then $Z(\alpha, \varepsilon) \in [0, 1]$, which allows us to interpret Z as a probability.

D. Asymptotic growth of the anomalous dimension

For the 4-dimensional physical model, ansatz (8.7) delivers the growth parameters

$$\begin{aligned}
\lambda = \frac{1}{s}, \quad \beta(s) = -\frac{3+2s}{s}, \quad b^{(1)}(s) &= -\frac{1+4s+3s^2}{s}, \\
b^{(2)}(s) &= \frac{1+6s+8s^2-2s^3-5s^4}{2s^2}, \\
b^{(3)}(s) &= \frac{-1-6s-s^2+24s^3-25s^4-126s^5-81s^6}{6s^3}.
\end{aligned} \tag{D.1}$$

They match [9, (14)] for $s = -2$. For the 6-dimensional physical model, there are three solutions:

$$\begin{aligned}
\vec{\lambda}(s) &= \Big(-\frac{6}{s}, -\frac{12}{s}, -\frac{18}{s}\Big), \quad \vec{\beta}(s) = \Big(-\frac{35+29s}{6s}, -\frac{5+2s}{3s}, -\frac{15+13s}{2s}\Big), \\
\vec{b}^{(1)}(s) &= \Big(\frac{-275-267s+8s^2}{216s}, \frac{265+624s+359s^2}{108s}, \frac{85+241s+156s^2}{72s}\Big), \\
\vec{b}^{(2)}(s) &= \Big(\frac{75625+83790s-101849s^2-177828s^3-67814s^4}{93312s^2}, \\
&\qquad \frac{70225+339690s+602764s^2+465258s^3+131959s^4}{23328s^2}, \\
&\qquad \frac{7225+37950s+69779s^2+51628s^3+12574s^4}{10368s^2}\Big), \\
\vec{b}^{(3)}(s) &= \Big(\frac{1}{60466176s^3}\cdot(-20796875-8551125s+107422197s^2+206297091s^3 \\
&\qquad +177713418s^4+90251478s^5+23658704s^6), \\
&\qquad \frac{1}{7558272s^3}(18609625+138592350s+424432473s^2+687305592s^3 \\
&\qquad +624311121s^4+303609366s^5+62154089s^6), \\
&\qquad \frac{1}{2239488s^3}(614125+4453575s+12499453s^2+16989843s^3 \\
&\qquad +11830354s^4+4259034s^5+758520s^6)\Big).
\end{aligned} \tag{D.2}$$

Including order $1/n^3$, the large-order growth of c_n is determined entirely by the first component of these vectors. In order to match [10, (41)–(43)], $b^{(1)}$ has to be multiplied with 3, $b^{(2)}$ with 9 and $b^{(3)}$ with 27. Parameters for the toy model are given in Table 11 in Appendix E.

E. Tables

s	$\gamma(\alpha)$
5	$-\alpha - 6\alpha^2 - 102\alpha^3 - 2640\alpha^4 - 87804\alpha^5 - 3483072\alpha^6 - 158329512\alpha^7 - 8050087584\alpha^8$
4	$-\alpha - 5\alpha^2 - 70\alpha^3 - 1485\alpha^4 - 40370\alpha^5 - 1306370\alpha^6 - 48365100\alpha^7 - 2000065725\alpha^8$
3	$-\alpha - 4\alpha^2 - 44\alpha^3 - 728\alpha^4 - 15368\alpha^5 - 384960\alpha^6 - 11004672\alpha^7 - 350628096\alpha^8$
2	$-\alpha - 3\alpha^2 - 24\alpha^3 - 285\alpha^4 - 4284\alpha^5 - 75978\alpha^6 - 1530720\alpha^7 - 34237485\alpha^8$
1	$-\alpha - 2\alpha^2 - 10\alpha^3 - 72\alpha^4 - 644\alpha^5 - 6704\alpha^6 - 78408\alpha^7 - 1008480a^8$
0	$-\alpha - \alpha^2 - 2\alpha^3 - 5\alpha^4 - 14\alpha^5 - 42\alpha^6 - 132\alpha^7 - 429\alpha^8$
−1	$-\alpha$
−2	$-\alpha + \alpha^2 - 4\alpha^3 + 27\alpha^4 - 248\alpha^5 + 2830\alpha^6 - 38232\alpha^7 + 593859\alpha^8$
−3	$-\alpha + 2\alpha^2 - 14\alpha^3 + 160\alpha^4 - 2444\alpha^5 + 45792\alpha^6 - 1005480\alpha^7 + 25169760\alpha^8$
−4	$-\alpha + 3\alpha^2 - 30\alpha^3 + 483\alpha^4 - 10314\alpha^5 + 268686\alpha^6 - 8167068\alpha^7 + 281975715\alpha^8$
−5	$-\alpha + 4\alpha^2 - 52\alpha^3 + 1080\alpha^4 - 29624\alpha^5 + 988288\alpha^6 - 38377152\alpha^7 + 1689250176\alpha^8$

Table 6. Non-linear DSE in $D = 4$ dimensions, see Section 8.2. Series expansion of the anomalous dimension in MOM as a function of the renormalized coupling α up to order α^8 for various powers s of the invariant charge $Q = G^s$. Only insertions into a single internal edge were performed in all cases.

s	$S(s)$
5	−0.025296711447842155554062589810922604262477942805771
4	−0.027093755285804302538145834438779321901953254099492
3	−0.027514268695235967509951466619196206136028416088749
2	−0.022754314527304604570864961094569471756231077114904
1	−0.005428317993266202636748034138132075286101589263688 3
−2	0.207553748710297351670134124720668682684453514969 63
−3	0.129235675811091778715229366859663994914292887084 30
−4	0.087977369959821254076048394021324447743442962588612
−5	0.065314016354658749144010387750377100215558556707446

Table 7. First 50 digits of the Stokes constant $S(s)$ for the non-linear DSE in $D = 4$, see equation (8.8). One finds $S(-2) = (\sqrt{\pi}e)^{-1}$ and $S(-3) = 3(\sqrt{\pi}e)^{-2}$.

s	$\ln \overline{\delta}(\alpha)$	f_{n+1}/f_n
5	$-2 - 9\alpha + (-139 + 14\zeta(3))\alpha^2 + (-3464 - \frac{7\pi^4}{12} + 233\zeta(3))\alpha^3$	30.22 ± 0.09
4	$-2 - \frac{15}{2}\alpha + (-\frac{575}{6} + 10\zeta(3))\alpha^2 + (-\frac{23525}{12} - \frac{\pi^4}{3} + \frac{410}{3}\zeta(3))\alpha^3$	25.09 ± 0.06
3	$-2 - 6\alpha + (-\frac{182}{3} + \frac{20}{3}\zeta(3))\alpha^2 + (-\frac{2911}{3} - \frac{\pi^4}{6} + \frac{214}{3}\zeta(3))\alpha^3$	19.96 ± 0.04
2	$-2 - \frac{9}{2}\alpha + (\frac{-67}{2} + 4\zeta(3))\alpha^2 + (-\frac{773}{2} - \frac{\pi^4}{15} + 31\zeta(3))\alpha^3$	14.80 ± 0.02
1	$-2 - 3\alpha + (-\frac{43}{3} + 2\zeta(3))\alpha^2 + (-\frac{305}{3} - \frac{\pi^4}{60} + \frac{29}{3}\zeta(3))\alpha^3$	9.60 ± 0.01
0	$-2 - \frac{3}{2}\alpha + (-\frac{19}{6} + \frac{2}{3}\zeta(3))\alpha^2 + (-\frac{103}{12} + \frac{4}{3}\zeta(3))\alpha^3$	
-1	-2	
-2	$-2 + \frac{3}{2}\alpha - \frac{29}{6}\alpha^2 + (\frac{94}{3} - \frac{1}{3}\zeta(3))\alpha^3$	5.8 ± 1.8
-3	$-2 + 3\alpha + (-\frac{53}{3} + \frac{2}{3}\zeta(3))\alpha^2 + (\frac{578}{3} + \frac{\pi^4}{60} - \frac{17}{3}\zeta(3))\alpha^3$	10.50 ± 0.11
-4	$-2 + \frac{9}{2}\alpha + (-\frac{77}{2} + 2\zeta(3))\alpha^2 + (\frac{2365}{4} + \frac{\pi^4}{15} - 22\zeta(3))\alpha^3$	15.69 ± 0.05
-5	$-2 + 6\alpha + (-\frac{202}{3} + 4\zeta(3))\alpha^2 + (\frac{4003}{3} + \frac{\pi^4}{6} - \frac{166}{3}\zeta(3))\alpha^3$	20.85 ± 0.07

Table 8. Non-linear DSE in $D = 4$ dimensions. Here $\ln \overline{\delta}(\alpha)$ is the logarithm of the shift in the renormalization point between MOM- and MS-scheme (3.2). Shown are the first terms of its perturbative power series. Ratio f_{n+1}/f_n is the growth rate of the function $f(\alpha)$ in equation (8.14).

s	$10^6 \cdot S(s)$
5	$-48.879979612936267148575174247043686402701421680529$
4	$-33.683126435179258367949154667346857343063662040223$
3	$-16.197057487106552084835982615789341267879644562145$
2	$-2.874931066358404169842007765677311801515635631211 6$
1	$-0.005037643852252104613165864641040152093341435216 5372$
-2	$87595.552909179124483795447421262990627388017406822$
-3	$17853.256793175269493347991077950813245133374820922$
-4	$6637.593110037931650951894178458603722595701766 4650$
-5	$3384.186761682513227965148628942508807465013504 3176$

Table 9. First 50 digits of the Stokes constant $S(s)$ for $D = 6$, see equation (8.8).

s	$\ln \delta(\alpha)$
5	$-\frac{8}{3}+\frac{61}{24}\alpha+(-\frac{80213}{7776}+\frac{7}{18}\zeta(3))\alpha^2+(\frac{8813575}{139968}+\frac{7\pi^4}{2592}-\frac{2563}{1296}\zeta(3))\alpha^3$
4	$-\frac{8}{3}+\frac{305}{144}\alpha+(-\frac{331345}{46656}+\frac{5}{18}\zeta(3))\alpha^2+(\frac{119812205}{3359232}+\frac{\pi^4}{648}-\frac{2255}{1944}\zeta(3))\alpha^3$
3	$-\frac{8}{3}+\frac{61}{36}\alpha+(-\frac{52325}{11664}+\frac{5}{27}\zeta(3))\alpha^2+(\frac{14842891}{839808}+\frac{\pi^4}{1296}-\frac{1177}{1944}\zeta(3))\alpha^3$
2	$-\frac{8}{3}+\frac{61}{48}\alpha+(-\frac{38381}{15552}+\frac{1}{9}\zeta(3))\alpha^2+(\frac{3947825}{559872}+\frac{\pi^4}{3240}-\frac{341}{1296}\zeta(3))\alpha^3$
1	$-\frac{8}{3}+\frac{61}{72}\alpha+(-\frac{24437}{23328}+\frac{1}{18}\zeta(3))\alpha^2+(\frac{1560359}{839808}+\frac{\pi^4}{12960}-\frac{319}{3888}\zeta(3))\alpha^3$
0	$-\frac{8}{3}+\frac{61}{144}\alpha+(-\frac{10493}{46656}+\frac{1}{54}\zeta(3))\alpha^2+(\frac{518095}{3359232}-\frac{11}{972}\zeta(3))\alpha^3$
-1	$-\frac{8}{3}$
-2	$-\frac{8}{3}-\frac{61}{144}\alpha-\frac{17395}{46656}\alpha^2+(-\frac{114361}{209952}+\frac{11}{3888}\zeta(3))\alpha^3$
-3	$-\frac{8}{3}-\frac{61}{72}\alpha+(\frac{31339}{23328}+\frac{1}{54}\zeta(3))\alpha^2+(-\frac{359005}{104976}-\frac{\pi^4}{12960}+\frac{187}{3888}\zeta(3))\alpha^3$
-4	$-\frac{8}{3}-\frac{61}{48}\alpha+(-\frac{45283}{15552}+\frac{1}{18}\zeta(3))\alpha^2+(-\frac{11830593}{1119744}-\frac{\pi^4}{3240}+\frac{121}{648}\zeta(3))\alpha^3$
-5	$-\frac{8}{3}-\frac{61}{36}\alpha+(-\frac{59227}{11664}+\frac{1}{9}\zeta(3))\alpha^2+(-\frac{20089615}{839808}-\frac{\pi^4}{1296}+\frac{913}{1944}\zeta(3))\alpha^3$

Table 10. First perturbative coefficients of $\ln \delta(\alpha)$ for $D = 6$ dimensions.

s	$S(s)$	$b^{(1)}(s)$	$b^{(2)}(s)$
5	−0.32358439814031030546	−33.713129682396588961	565.374787298670
4	−0.39133508371923490586	−28.505508252042547410	405.630022359080
3	−0.48873615802624779599	−23.352717957250113407	273.573399332400
2	−0.62073652944344889658	−18.337005501361698274	169.862094180663
1	−0.59543401151910843904	−13.869604401089358619	98.0525675224480
−2	0.63661977236758134308	4.4674011002723396547	7.97883629535726
−3	0.52618629546780378450	9.4831135561607547882	40.2545894932164
−4	0.41925649525660905756	14.635903850953188791	98.9744451682625
−5	0.34358721547093244258	19.843525281307230343	184.621956597118

Table 11. First digits of the Stokes constant $S(s)$ and subleading corrections of the asymptotic growth (8.8) of the anomalous dimension in the toy model of Section 10.

s	$\alpha \ln \overline{\delta}(\alpha(A))$
5	$-6A - \frac{2009}{3}A^2 - \frac{11563106}{45}A^3 - \frac{173306477104}{945}A^4 - \frac{1228737945883358}{6075}A^5$ $- \frac{46235332362117842849}{147015}A^6$
4	$-5A - \frac{1130}{3}A^2 - \frac{4316822}{45}A^3 - \frac{59632972484}{1323}A^4 - \frac{461687074578658}{14175}A^5$ $- \frac{34025588969113725668}{1029105}A^6$
3	$-4A - \frac{554}{3}A^2 - \frac{1263424}{45}A^3 - \frac{10282878575}{1323}A^4 - \frac{46540947260036}{14175}A^5$ $- \frac{398737839692532122}{205821}A^6$
2	$-3A - \frac{217}{3}A^2 - \frac{1233338}{225}A^3 - \frac{4881119933}{6615}A^4 - \frac{3528108924854}{23625}A^5$ $- \frac{1074400592111547046}{25727625}A^6$
1	$-2A - \frac{55}{3}A^2 - \frac{106898}{225}A^3 - \frac{135875429}{6615}A^4 - \frac{272890120256}{212625}A^5$ $- \frac{2770658834393158}{25727625}A^6$
0	$-A - \frac{4}{3}A^2 - \frac{146}{45}A^3 - \frac{8864}{945}A^4 - \frac{417682}{14175}A^5 - \frac{9095176}{93555}A^6$
-1	0
-2	$A + 7A^2 + 242A^3 + 17771A^4 + 2189294A^5 + 404590470A^6$
-3	$2A + 41A^2 + \frac{92518}{25}A^3 + \frac{503885698}{735}A^4 + \frac{1639676026462}{7875}A^5$ $+ \frac{266517331818761291}{2858625}A^6$
-4	$3A + \frac{370}{3}A^2 + \frac{4782122}{225}A^3 + \frac{48904622516}{6615}A^4 + \frac{887103429351554}{212625}A^5$ $+ \frac{886009137176955955 72}{25727625}A^6$
-5	$4A + \frac{826}{3}A^2 + \frac{3478864}{45}A^3 + \frac{287007344207}{6615}A^4 + \frac{185545372999796}{4725}A^5$ $+ \frac{53252838327756373006}{1029105}A^6$

Table 12. First coefficients of $\ln \delta(\alpha)$ in the toy model of Section 10, up to order α^{11}. Here, $A := (\alpha\pi)^2/4$.

Acknowledgments. The author thanks Dirk Kreimer, David Broadhurst and Gerald Dunne for several helpful discussions and for comments and suggestions on the draft.

References

[1] I. Aniceto, G. Başar, and R. Schiappa, A primer on resurgent transseries and their asymptotics. *Phys. Rep.* **809** (2019), 1–135 MR 3955133

[2] E. T. Bell, Exponential polynomials. *Ann. of Math. (2)* **35** (1934), no. 2, 258–277 Zbl 0009.21202 MR 1503161

[3] M. P. Bellon, Approximate differential equations for renormalization group functions in models free of vertex divergencies. *Nuclear Phys. B* **826** (2010), no. 3, 522–531 Zbl 1203.81123 MR 2559550

[4] M. P. Bellon, An efficient method for the solution of Schwinger–Dyson equations for propagators. *Lett. Math. Phys.* **94** (2010), no. 1, 77–86 Zbl 1198.81147 MR 2720256

[5] M. P. Bellon and F. A. Schaposnik, Renormalization group functions for the Wess–Zumino model: up to 200 loops through Hopf algebras. *Nuclear Phys. B* **800** (2008), no. 3, 517–526 Zbl 1292.81101 MR 2424589

[6] C. G. Bollini and J. J. Giambiagi, Dimensional renormalization: the number of dimensions as a regularizing parameter. *Nuovo Cim. B* **12** (1972), no. 1, 20–26

[7] K. Bönisch, F. Fischbach, A. Klemm, C. Nega, and R. Safari, Analytic structure of all loop banana amplitudes. *J. High Energy Phys.* **2021** (2021), no. 5, paper no. 66 Zbl 1466.81022

[8] M. Borinsky, Generating asymptotics for factorially divergent sequences. *Electron. J. Combin.* **25** (2018), no. 4, paper no. 4.1 Zbl 1398.05034 MR 3874267

[9] M. Borinsky and G. V. Dunne, Non-perturbative completion of Hopf-algebraic Dyson–Schwinger equations. *Nuclear Phys. B* **957** (2020), paper no. 115096 Zbl 1473.81123 MR 4118920

[10] M. Borinsky, G. V. Dunne, and M. Meynig, Semiclassical trans-series from the perturbative Hopf-algebraic Dyson–Schwinger equations: ϕ^3 QFT in 6 dimensions. *SIGMA Symmetry Integrability Geom. Methods Appl.* **17** (2021), paper no. 087 Zbl 1480.81096 MR 4316586

[11] D. J. Broadhurst and D. Kreimer, Combinatoric explosion of renormalization tamed by Hopf algebra: 30-loop Padé–Borel resummation. *Phys. Lett. B* **475** (2000), no. 1–2, 63–70 Zbl 1049.81569 MR 1748409

[12] D. J. Broadhurst and D. Kreimer, Exact solutions of Dyson–Schwinger equations for iterated one-loop integrals and propagator-coupling duality. *Nuclear Phys. B* **600** (2001), no. 2, 403–422 Zbl 1043.81049

[13] F. Brown and D. Kreimer, Angles, scales and parametric renormalization. *Lett. Math. Phys.* **103** (2013), no. 9, 933–1007 Zbl 1273.81164 MR 3077961

[14] C. G. Callan, Broken scale invariance in scalar field theory. *Phys. Rev. D* **2** (1970), no. 8, 1541–1547

[15] W. Celmaster and R. J. Gonsalves, Renormalization-prescription dependence of the quantum-chromodynamic coupling constant. *Phys. Rev. D* **20** (1979), no. 6, 1420–1434

[16] J. C. Collins and A. J. Macfarlane, New methods for the renormalization group. *Phys. Rev. D* **10** (1974), no. 4, 1201–1212

[17] L. Comtet, *Advanced combinatorics. the art of finite and infinite expansions*. enlarged edn., D. Reidel Publishing Co., Dordrecht, 1974 Zbl 0283.05001 MR 0460128

[18] A. Connes and D. Kreimer, Renormalization in quantum field theory and the Riemann–Hilbert problem. II. The β-function, diffeomorphisms and the renormalization group. *Comm. Math. Phys.* **216** (2001), no. 1, 215–241 Zbl 1042.81059 MR 1810779

[19] A. Connes and M. Marcolli, *Noncommutative geometry, quantum fields and motives*. Amer. Math. Soc. Colloq. Publ. 55, American Mathematical Society, Providence, RI, 2008 Zbl 1209.58007 MR 2371808

[20] J. Courtiel and K. Yeats, Next-to^k leading log expansions by chord diagrams. *Comm. Math. Phys.* **377** (2020), no. 1, 469–501 Zbl 1447.81169 MR 4107935

[21] L. Delage, Leading log expansion of combinatorial Dyson Schwinger equations. 2016, arXiv:1602.08705

[22] R. Delbourgo, D. Elliott, and D. S. McAnally, Dimensional renormalization in ϕ^3 theory: Ladders and rainbows. *Phys. Rev. D* **55** (1977), no. 8, 5230–5233

[23] R. Delbourgo, A. C. Kalloniatis, and G. Thompson, Dimensional renormalization: ladders and rainbows. *Phys. Rev. D* **54** (1976), no. 8, 5373–5376

[24] F. J. Dyson, The S matrix in quantum electrodynamics. *Phys. Rev.* **75** (1949), no. 11, 1736–1755 Zbl 0033.14201 MR 31388

[25] D. J. Gross, Applications of the renormalization group to high-energy physics. In *Methods in field theory (Les Houches, 1975)*, pp. 141–250, North-Holland, Amsterdam, 1976

[26] L. Klaczynski, *Haag's theorem in renormalised quantum field theories*. Ph.D. thesis, 2016, Humbold-Universität zu Berlin, DOI 10.18452/17448, arXiv:1602.00662

[27] L. Klaczynski, Resurgent transseries & Dyson–Schwinger equations. *Ann. Physics* **372** (2016), 397–448 Zbl 1380.81236 MR 3541607

[28] D. Kreimer, Chen's iterated integral represents the operator product expansion. *Adv. Theor. Math. Phys.* **3** (1999), no. 3, 627–670 Zbl 0971.81093 MR 1797019

[29] D. Kreimer, Étude for linear Dyson–Schwinger equations. In *Traces in number theory, geometry and quantum fields*, pp. 155–160, Aspects Math. E38, Friedr. Vieweg, Wiesbaden, 2008 Zbl 1146.81040 MR 2427594

[30] D. Kreimer and E. Panzer, Renormalization and Mellin transforms. In *Computer algebra in quantum field theory*, pp. 195–223, Texts Monogr. Symbol. Comput., Springer, Vienna, 2013 Zbl 1308.81137 MR 3616752

[31] D. Kreimer and K. Yeats, An étude in non-linear Dyson–Schwinger equations. *Nuclear Phys. B Proc. Suppl.* **160** (2006), 116–121 MR 2255485

[32] O. Krüger, Log expansions from combinatorial Dyson–Schwinger equations. *Lett. Math. Phys.* **110** (2020), no. 8, 2175–2202 Zbl 1446.81032 MR 4126877

[33] O. Krüger and D. Kreimer, Filtrations in Dyson–Schwinger equations: next-to$^{\{j\}}$-leading log expansions systematically. *Ann. Physics* **360** (2015), 293–340 Zbl 1360.81244 MR 3367538

[34] G. Mack and I. T. Todorov, Conformal-invariant green functions without ultraviolet divergences. *Phys. Rev. D* **8** (1973), no. 6, 1764–1787

[35] A. J. McKane, Perturbation expansions at large order: Results for scalar field theories revisited. *J. Phys. A* **52** (2019), no. 2, paper no. 055401 Zbl 1422.81146

[36] The on-line encyclopedia of integer sequences. https://oeis.org

[37] E. Panzer, Hopf algebraic renormalization of Kreimer's toy model. 2012, arXiv:1202.3552

[38] E. Panzer, Renormalization, Hopf algebras and Mellin transforms. In *Feynman amplitudes, periods and motives*, pp. 169–202, Contemp. Math. 648, American Mathematical Society, Providence, RI, 2015 Zbl 1346.81102 MR 3415415

[39] L. F. Richardson, The approximate arithmetical solution by finite differences of physical problems involving differential equations, with an application to the stresses in a masonry dam. *Phil. Trans. R. Soc. Lond. A* **210** (1911), no. 459–470, 307–357

[40] J. Schwinger, On the Green's functions of quantized fields. I, II. *Proc. Natl. Acad. Sci. USA* **37** (1951), 452–459 MR 45065

[41] K. Symanzik, Small distance behaviour in field theory and power counting. *Comm. Math. Phys.* **18** (1970), no. 3, 227–246 Zbl 0195.55902 MR 1552571

[42] G. 't Hooft, Dimensional regularization and the renormalization group. *Nuclear Phys. B* **61** (1973), 455–468

[43] G. 't Hooft and M. Veltman, Regularization and renormalization of gauge fields. *Nuclear Phys. B* **44** (1972), no. 1, 189–213 MR 391798

[44] K. Yeats, *Growth estimates for Dyson–Schwinger equations*. Ph.D. thesis, 2008, Boston University, arXiv:0810.2249

[45] K. Yeats, Rearranging Dyson–Schwinger equations (with a foreword by Dirk Kreimer). *Mem. Amer. Math. Soc.* **211** (2011), no. 995 Zbl 1221.81005 MR 2791969

Communicated by Frédéric Patras

Received 31 January 2022; revised 10 June 2022.

Paul-Hermann Balduf
Institut für Physik, Humboldt-Universität zu Berlin, Newtonstraße 15, 12489 Berlin, Germany; current address: Department of Combinatorics and Optimization, University of Waterloo, ON N2L 3G1, Canada; pbalduf@uwaterloo.ca